INTERNATIONAL UNIVERSITY LIAISON INDONESIA

BACHELOR'S THESIS

EFFECT OF DIFFERENT HYBRIDIZATION LEVEL ON ATR 72 RANGE PERFORMANCE

By

Reyhan Athalla

11201901004

Presented to the Faculty of Engineering

In Partial Fulfilment Of the Requirements for the Degree of

SARJANA TEKNIK

In

AVIATION ENGINEERING

FACULTY OF ENGINEERING

BSD City 15345

Indonesia

February 2023

APPROVAL PAGE

EFFECT OF DIFFERENT HYBRIDIZATION LEVEL ON ATR 72 RANGE PERFORMANCE

REYHAN ATHALLA
11201901004
Presented to the Faculty of Engineering
In Partial Fulfillment of the Requirements for the Degree of

SARJANA TEKNIK
In
AVIATION ENGINEERING

FACULTY OF ENGINEERING

Triwanto Simanjuntak, PhD	________
Thesis Advisor	Date
Dr. Eng. Ressa Octavianty	________
Thesis Co-Advisor	Date
Dipl.-Ing. Wahjoe Goeritno, M.Si.	________
Dean of Faculty of Engineering	Date

EXAMINERS APPROVAL PAGE

Dr. Ir. Erie Sandhita	____________________
Examiner 1	Date
Ir. Setyo Utomo Soekarsono M.Sc., M.M.	____________________
Examiner 2	Date

STATEMENT BY THE AUTHOR

I hereby declare that this submission is my own work and to the best of my knowledge, it contains no material previously published or written by another person, nor material which to a substantial extent has been accepted for the award of any other degree or diploma at any educational institution, except where due acknowledgement is made in the thesis.

Reyhan Athalla	
Student	Date

ABSTRACT

Effect of Different Hybridization Level on ATR 72 Range Performance

by

Reyhan Athalla

Triwanto Simanjuntak, PhD, Advisor
Dr. Eng. Ressa Octavianty, Co-Advisor

This thesis presents the range performance analysis of ATR72-X that converted into Hybrid-Electrical Aircraft under various hybridization factors such as Hybridization of Power (H_p) and Hybridization of Energy (H_E), also with the various battery specific energy. This thesis's primary problem is finding and verifying the formulation in calculating the range of hybrid-electric propulsion aircraft. Then we analyze the range performance concerning the hybridization factors and various battery-specific energy. For this study, the MTOW of the aircraft are assumed to be constant from the reference aircraft. The results show that with the increase of H_P for the constant MTOW, the aircraft range is also increasing, but as the H_E increases, the aircraft range will decrease instead. With the various specific energy, the range of aircraft will also increase as it increases. With present technological advancement, achieving a range comparable to the conventional configuration is still quite challenging. However, based on the results, it is achievable for the 740 km range using H_P of around 0.4 and H_E of about 0.1 for 500 Wh/kg specific battery energy. Overall, it is possible to convert the aircraft to Hybrid-Electrical without changing any configuration to the aircraft's overall weight, but it would need much more technological advances.

Keyword: *Hybrid-Electric propulsion, Range Performance,*

ACKNOWLEDGEMENTS

I would like to express my sincerest gratitude to all those who have supported and encourage me throughout the entire process and completion of this thesis.

First and foremost, praises and thanks to Allah, the Almighty, for his showers and blessing throughout this thesis and give me health, patience, and knowledge upon the completion of this thesis.

I would like to extend my heartfelt thanks to my thesis advisor and co-advisor, Triwanto Simanjuntak, PhD and Dr. Eng. Ressa Octavianty, for the invaluable guidance, support, and encouragement throughout the entire research process. Their invaluable insights, feedback, and knowledge helped me in shaping me and this thesis into a better form. And even when I am down and not motivated, they always get me back in shape and keeps me motivated to complete my thesis. I cannot thank them enough for giving me their time and efforts to help me and be my advisors for this thesis, even though they had so many other activities and affairs.

I would like to extend my gratitude to my colleagues and friends who provided me with their support and encouragement during challenging times. Their support also keeps me motivated and focus on this thesis and completing it.

Lastly, I would like to express my gratitude to my family, especially my parents, for their constant love, support, and encouragement in any kind of form. Their sacrifice and belief in me have been crucial in enabling me to reach this stage in my life and academic journey.

I am grateful to everyone who has contributed, in one way or another, to the completion of this thesis. This achievement would not have been possible without the support and encouragement of all those who have believed in me. Thank you all for your incredible, invaluable support and contribution.

Contents

List of Figures

List of Tables

List of Abbreviations

BED	**B**attery **E**nergy **D**ensity
DESPPS	**D**ual **E**nergy **S**torage **P**ropulsion **P**ower **S**ystem
DoH	**D**egree **o**f **H**ybridization
EIS	**E**ntry **I**nto **S**ervice
HEPS	**H**ybrid **E**lectrical **P**ropulsion **S**ystem
ICE	**I**nternal **C**ombustion **E**ngine
MEA	**M**ore **E**lectric **A**aircraft
MTOW	**M**aximum **T**ake **O**ff **W**eight
TRL	**T**echnology **R**eadiness **L**evel

List of Symbols

Symbol	Unit	Name
ρ	kg/m^3	Atmoshperic density
η_p	-	Propeller efficiency
η_j	-	Propulsive efficiency
η_{electric}	-	Electrical efficiency
Φ	-	Supplied rower ratio
γ	-	Flight-path angle
AR	-	Aspect Ratio
C_P	m^{-1}	Specific fuel consumption for propeller driven aircraft
C_D	-	Coefficient of drag
C_{D_n}	-	Coefficient component drag
C_{D_0}	-	Zero-lift drag coefficient
C_L	-	Coefficient of Lift
CL/CD		Lift-drag ratio
D	-	Drag
D_w	-	Wing drag
D_n	-	Component drag
D_i	-	Induced drag
d_p	m	Propeller diameter
e	-	Oswald's efficiency factor
E_{bat}	J	Battery energy
E_{fuel}	J	Fuel energy
E_{start}	J	Starting energy
g	m/s^2	Gravitational acceleration
H_P	-	Hybridization of power (S)
H_E	-	Hybridization of energy (ψ)

H_{bat}	Wh/kg	Battery specific energy
H_{fuel}	Wh/kg	Fuel specific energy
k	-	Induced drag factor
M	-	Mach number
m_{bat}	kg	Battery mass
m_{fuel}	kg	fuel mass
P	W ($\mathrm{J\,s^{-1}}$)	Power
P_a	W ($\mathrm{J\,s^{-1}}$)	Power available
P_{br}	W ($\mathrm{J\,s^{-1}}$)	Shaft power
P_{em}	W ($\mathrm{J\,s^{-1}}$)	Power electric motor
P_r	W ($\mathrm{J\,s^{-1}}$)	Power required
Re	-	Reynolds number
R	km	Range
$R_{\max}$	km	Range maximum
R_{Hybrid}	km	Range hybrid-electric
S	m^2	Surface
T	N	Thrust
t	s	Time
V	m/s	Velocity
W	N	Weight

Dedicated to my parents

CHAPTER 1
INTRODUCTION

1.1 Background

The aviation sector has a long history of invention, and it has played an important part in shaping modern civilization by making air travel faster, safer, and more reliable. However, as the industry has changed, so have the challenges that aviation companies face. One major challenge facing the industry in the 21st century is addressing climate change, which can only be done by reducing the environmental impact of airplanes. The main goal of this effort is to reduce the fuel needed for normal missions. This will make the planes lighter and save money for the companies.

1.1.1 Climate Change

Climate change is one of the most urgent issues confronting our planet today. Global temperatures have risen since the late 1800s, as seen in Figure 1.1, with the previous few decades being the warmest on record. Human activities, such as using fossil fuels, have contributed significantly to an increase in greenhouse gases, such as carbon dioxide, in the atmosphere. These gases trap heat from the sun, warming the Earth's surface and creating a variety of consequences, like rising sea levels, extreme weather events, and changes in the distribution of plant and animal species.

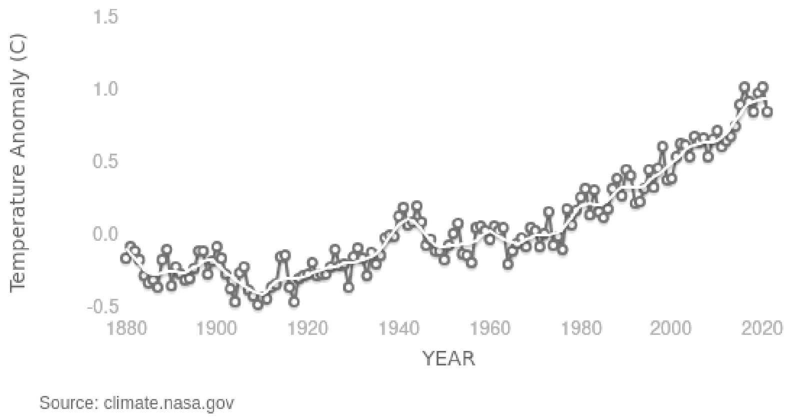

FIGURE 1.1: Temperature since 1800s **nasa_nasa_2023**

Figure 1.2 depicts the growth in carbon dioxide (CO_2) concentration in the atmosphere over the last century. The concentration has increased over the previous few decades, with levels presently higher than at any point in the last 800,000 years. This trend is expected to continue unless drastic measures to reduce emissions and limit the pace of climate change are taken.

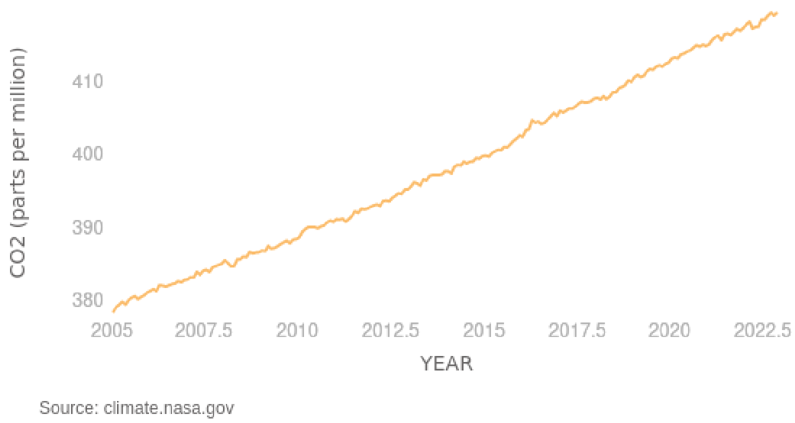

FIGURE 1.2: CO2 graph **nasa_nasa_2023**

1.1.2 Aviation Industry

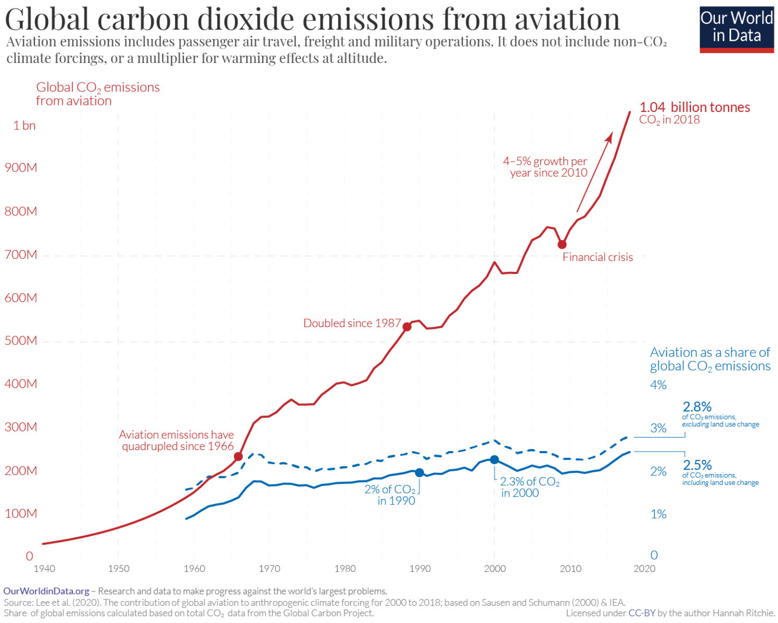

FIGURE 1.3: Global aviation Carbon Dioxide **ritchie_climate_2020**

The aviation industry is responsible for around 2–3 percent of global greenhouse gas emissions and is one of the fastest-growing sources of emissions. Jet fuel, which is used to power the majority of commercial aircraft, is a significant source of carbon dioxide emissions. Additionally, aircraft engines release other greenhouse gases, such as water vapor and nitrous oxide, which contribute to the warming of the atmosphere.

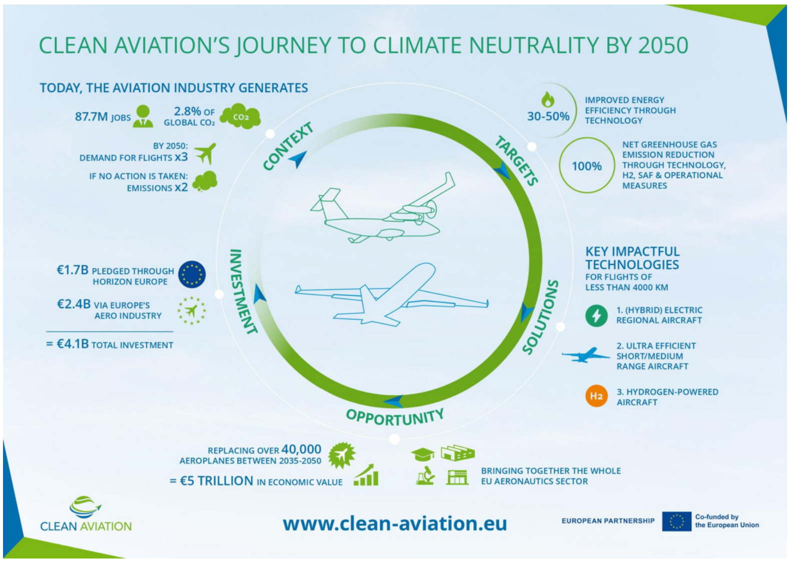

FIGURE 1.4: Clean Aviation infographic **clean__aviation__infographic__2023**

Figure 1.3 illustrates the increased carbon dioxide emissions from the aviation sector over the past few decades. It is clear that emissions have risen sharply, and the trend is expected to continue if urgent action is not taken to reduce emissions and slow the pace of climate change.

1. Sustainable alternative fuels: One of the most promising solutions is to use sustainable alternative fuels, such as biofuels made from algae or waste products, to power aircraft. These fuels have a lower carbon footprint than traditional jet fuel and can significantly reduce emissions **noauthor__gfaaf__nodate**;

2. Operational efficiency: Airlines can also reduce emissions by improving the efficiency of their operations. This can be achieved by optimizing flight routes, reducing taxi times, and reducing weight on board **mccausland__net__2022**;

3. Carbon offsetting: Carbon offsetting is another approach that allows airlines to offset their emissions by investing in projects that reduce or remove greenhouse gases from the atmosphere. This can be done through programs such as the Carbon Offsetting and Reduction Scheme for International Aviation (CORSIA) **noauthor__carbon__nodate**;

4. Technological advancement: Advancements in aircraft design and propulsion technology can also help to reduce emissions. For example, electric and hybrid aircraft are being developed that have the potential to reduce the carbon footprint of aviation significantly **clean_aviation_infographic_2023**;

5. International cooperation: International cooperation is important to establish regulations and agreements to limit greenhouse gas emissions from the aviation sector **noauthor_carbon_nodate**.

These solutions, along with a combination of other measures, can significantly reduce the impact of aviation on the environment and play a significant role in addressing the climate change problem.

1.1.3 More Electric Aircraft

Technological innovation, specifically More Electric Aircraft, is one solution to the aviation industry's challenge. A More Electric Aircraft (MEA) uses electric power for a more significant proportion of its systems and subsystems rather than hydraulic, pneumatic, or mechanical systems. This frequently involves the replacement of traditional mechanical and pneumatic actuators with electric actuators, as well as using electric motors to power systems such as pumps, generators, and fans. MEA also requires advanced power electronics and energy storage solutions, such as batteries.

The primary motivation for developing MEA technology is to improve the overall efficiency of the aircraft and reduce its environmental impact. The aircraft can be made lighter and more reliable by using electric power since electric systems are less complex than traditional mechanical systems. Additionally, electric power can improve fuel efficiency and reduce emissions **naayagi_review_2013**

The increased electrical power on board poses new challenges for aircraft design and operation, such as increased weight of power generation and energy storage, electrical power distribution and management, and thermal control.

Many major aircraft manufacturers are now working on MEA technology development, and several MEA demonstrators have already been developed and tested.

Examples of MEA systems include electric taxiing, electric braking, hybrid electric propulsion, fully electric propulsion, electric de-icing systems, electric bleed air systems, electric-hydraulic actuators, and electric-mechanical actuators.

This thesis focuses more on electric propulsion systems such as fully electric propulsion and hybrid electric propulsion. Fully electric propulsion, also known as all-electric propulsion, is a propulsion system in which electric motors powered by an energy storage system, such as batteries, are used to drive the aircraft's propulsion system. In contrast to hybrid electric propulsion, which uses electric motors and an internal combustion engine, fully electric propulsion does not use any internal combustion engine.

The main advantage of fully electric propulsion is that it can be highly efficient and significantly reduce emissions and noise compared to traditional internal combustion engines. Electric motors are more straightforward, lighter, and more reliable than internal combustion engines, and they can be more easily integrated into the aircraft's design **noauthor__electrical__nodate**

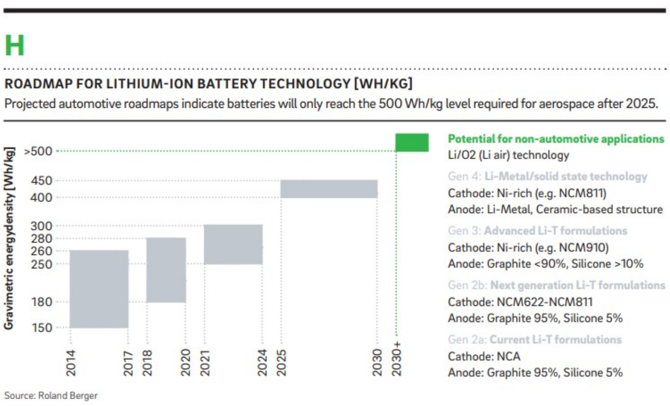

FIGURE 1.5: Roadmap for lithium battery **noauthor__new__nodate**

However, there are also some challenges associated with fully electric propulsion. The main problem is that batteries don't have as much energy per unit as traditional aviation fuels do. For it to be commercially viable, according to Roland Berger **noauthor__new__nodate**, the energy density of the storage needed at least 500 Wh/kg. In today's technology, the highest battery density available is up to 450 Wh/kg, which is the Amprius battery **noauthor__100__nodate**. The battery technology development will be needed to reach the 500 Wh/kg mark. However, it is still far away from the energy density that could be delivered by jet fuel with approximately 12 kWh/kg. This means that fully electric aircraft would require more extensive and heavier batteries to store enough energy to fly, increasing the aircraft's weight and decreasing its range. Additionally, fully electric aircraft would need to be recharged or have their batteries replaced more frequently than aircraft with internal combustion engines, which would require the development of new ground-based infrastructure and logistics.

Currently, fully electric propulsion is mainly used in small and regional aircraft, such as drones and eVTOL aircraft. Still, some companies and research organizations are working on developing fully electric propulsion for larger commercial aircraft.

The technology is still in its early stages of development and requires more research and development to overcome the challenges; future advances in battery technology and energy storage devices would be critical to making it more commercially viable.

Hybrid electric propulsion is a propulsion system that combines a traditional internal combustion engine (ICE) with one or more electric motors and an energy storage system, such as batteries. The electric motors are powered by the energy stored in the batteries, which can be charged by the internal combustion engine or from an external source, such as a ground-based electrical supply.

The main advantage of hybrid electric propulsion is that it can significantly improve the efficiency of the aircraft. The electric motors can provide additional power when the aircraft needs it, such as during takeoff and climb. At the same time, the internal combustion engine can run at optimal efficiency during the cruise. Additionally, electric motors can power the aircraft during taxi, reducing the need for ground-based power and reducing emissions.
Hybrid electric propulsion system can be categorized into several configurations:

- Series hybrid electric propulsion;
- Turboelectric;
- Serial/Parallel Hybrid Electric;
- Parallel hybrid electric propulsion.

In either case, electric motors and internal combustion engines are used together to provide optimal performance and efficiency. The electric motor can work as a generator, assist the internal combustion engine, or fly purely on electric power, depending on the aircraft's specific design, conditions, or flight phases.

Currently, there are few commercial examples of hybrid electric aircraft. Still, some companies and research organizations are testing hybrid-electric propulsion technologies in small and medium-sized aircraft. The technology is expected to continue to advance and become more widely adopted.

If more electric aircraft are implemented into the aviation market, we will definitely see an improvement in global carbon emissions.

1.1.4 Hybrid-Electric Concepts

The development of hybrid-electric concept aircraft has been going on for the past few years. NASA has classified the aircraft concepts into the categories of Technology Readiness Level (TRL), which are the scale of progressing levels of maturity. Some concepts are listed in the Table below **rendon_aircraft_2021**.

Name	EIS	Seats	TRL	Range	Status	Reference
hybrid E-fan X	2035	50-100	6-7	-	Cancelled	**kaminski-morrow_airbus_nodatenoauthor_e-fan_2021**
Eviation Alice	2027	9	6-7	300 km	-	**rains_one_nodateeviation_aircraft_2021**
Zunum ZA10 Aero	-	12	5-6	1127 km	Cancelled	**noauthor_zunum_nodate**
PEGASUS	2030	48	4-5	400 nm	Under Development	**sahoo_review_2020**
N3-X	2040-2045	300	3-4	13890	Under Development	**noauthor_n3-x_nodatefelder_nasa_nodate**
STARC-ABL	2035-2040	150	3-4	900 nm	-	**sahoo_review_2020noauthor_single-aisle_nodate**
Boeing SUGAR	2040	154	3-4	6482 km	-	**noauthor_how_nodate**
Wight-1	2035	186	3-4	460	-	**randall_wright_2022rendon_aircraft_2021**
ECO-150	2035	150	2-3	1650 nm	-	**noauthor_eco-150_nodatesahoo_review_2020**
VerdeGo Aero PAT200	-	2	2-3	-	-	**noauthor_our_nodate**
EAG HERA	2028	70	-	1482 km	Under Development	**alcock_eag_nodate**, **alcock_eviations_nodate**
Silent Air Taxi	2024	4+1	-	>500 km	Under Development	**noauthor_silent_nodate**
Faradair BEHA M1H	2026	18	-	1850 km	Under Development	**noauthor_e-hapi_nodatenoauthor_faradair_nodate**
Electra eSTOL	2027	9	-	740 km	Under Development	**index_advanced_nodate**
Dufour Aero 3	2026	8	-	1020 km	Under Development	**noauthor_aero3_nodate**

1.2 Problem Statement

The problem that is going to be discussed in this thesis is how the ATR72 will perform in terms of cruising performance under various factors if we convert the aircraft into a Hybrid-Electrical Propulsion system. The factor that is going to be used are the following;

- Under various energy hybridization (H_e);
- Under various power split (H_P);
- Under various specific energy of the battery (Wh/kg).

1.3 Research Objectives

The objectives of this research are to investigate:

- To verify the formula for cruising performance of hybrid electric propulsion (HEP) aircraft that have been formulated by Voskujil **voskuijl_analysis_2018**, but in his paper, the formulation is short and in terse, so in this thesis, the formula will be explained more in detail;
- To analyze the range performance of ATR72-X under various hybridization level (H_E and H_P) and also with various specific energy battery level.

1.4 Research Scope

The scope of this thesis will be the following;

- Only the range performance is investigated in this thesis;
- The data and configuration of the airplane that is going to be used in this thesis are modified ATR72 from Nita's dissertation **nita_aircraft_2008**;
- The configuration of the conversion of the airplane to hybrid-electrical propulsion (HEP) is not investigated in this thesis;

- The configuration of the hybrid electric ATR72 is assumed to be the same as the conventional configuration.
- In determining the range for cruising performance, a steady straight non-sideslipping unaccelerated flight profile is assumed. However, it does not reflect in real-world operation since the aircraft could be flying with many factors during the cruising phase and accounting for the changes in each individual component of the drag profile would be a time-consuming task, which is why the assumption was made;
- The technology level of battery performance is assumed for this thesis.

1.5 Significance of the Study

The results of this research are expected:

- The results of the study can be used to calculate the aircraft performance of hybrid-electrical propulsion (HEP) aircraft.

1.6 Thesis Structure

This thesis will be divided into five parts:

1. Introduction
2. Literature Review
3. Research Methodology
4. Results and Discussions
5. Conclusion and Recommendation

CHAPTER 2
LITERATURE REVIEW

2.1 Hybrid Electric Aircraft

A hybrid electric aircraft combines a conventional internal combustion engine and one or more electric motors, as mentioned in Chapter 1. In the hybrid-electric vehicle, there is something called hybridization, which is the synergy between the two power sources (i.e., battery and fuel). In a study conducted by Pornet and Isikveren, they had what they called the Degree-of-Hybridization (DoH), which expressed the percentage of the total required power from the electrical system, but they said that for the advanced Dual Energy Storage and Propulsion Power System (DESPPS), it was not suitable to be represented by one parametric descriptor. In another study, they found that DESPPS generally requires two descriptors: (1) hybridization at the energy source (ψ) and (2) hybridization at shaft power or power split (S). These two descriptors has been used in various studies and literature **voskuijl_analysis_2018**, **de_vries_preliminary_2019**, **finger_aircraft_2019**, **pornet_conceptual_2015** which can be defined as:

$$H_P = \frac{P_{\text{bat}}}{P} = S \tag{2.1}$$

$$H_E = \frac{E_{\text{bat}}}{E_{\text{total}}} = \psi \tag{2.2}$$

However, the power split can be different throughout the mission of the aircraft; thus, another parameter is introduced, which is supplied power ratio **voskuijl_analysis_2018**:

$$\Phi = \frac{\int P_{\text{br, electric}}}{\int P_{\text{br, total}}} \tag{2.3}$$

The supplied power ratio is defined as the total shaft power from the electric motor in relation to the overall shaft power and is integrated throughout the mission. A value of 0 denotes traditional aircraft, whereas a value of 1 denotes pure electric aircraft. But when using a constant power split, the supplied power ratio will be similar to the power split. Figure 2.1 shows an example of a Degree-of-Hybridization (DoH) for DESPPS.

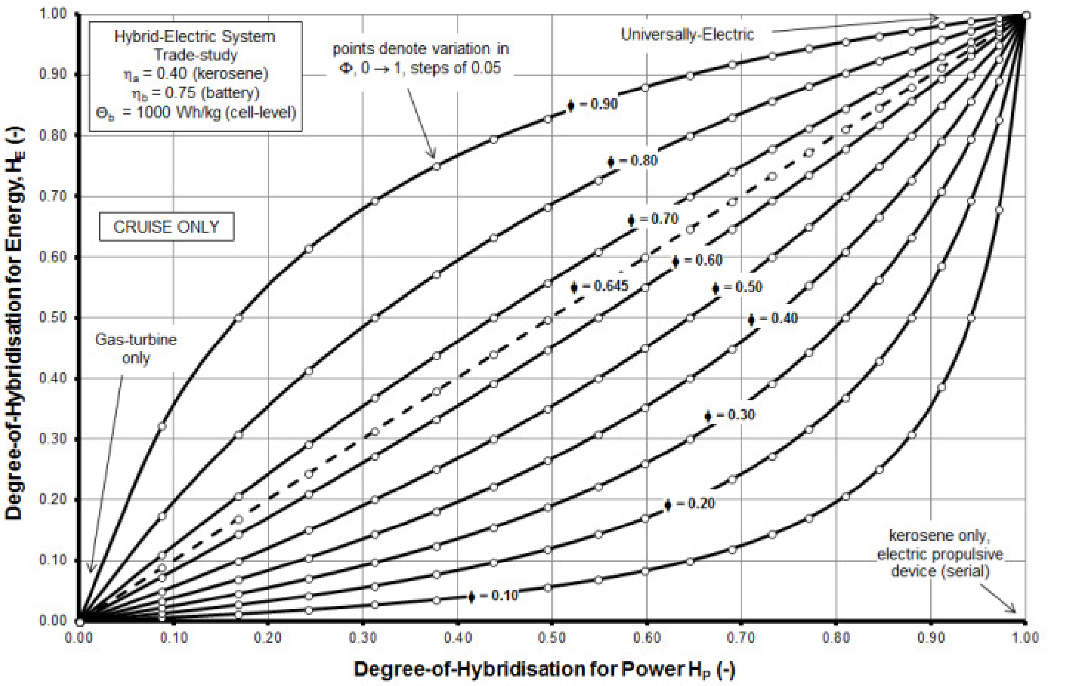

FIGURE 2.1: Example of a Degree-of-Hybridization trade-study conducted for a hypothetical DESPPS **pornet_conceptual_2015**

2.1.1 Hybrid electric architecture

TABLE 2.1: Classification of electric propulsion architectures

Architecture	H_P	H_E
Conventional	0	0
All-electric	1	1
Turboelectric	>0	0
Series Hybrid	1	<1
Parallel Hybrid	<1	<1

Table 2.1 categorizes electric propulsion architecture and conventional configurations in relation to hybridization factors. and Figure 2.2 shows the diagram of each architecture.

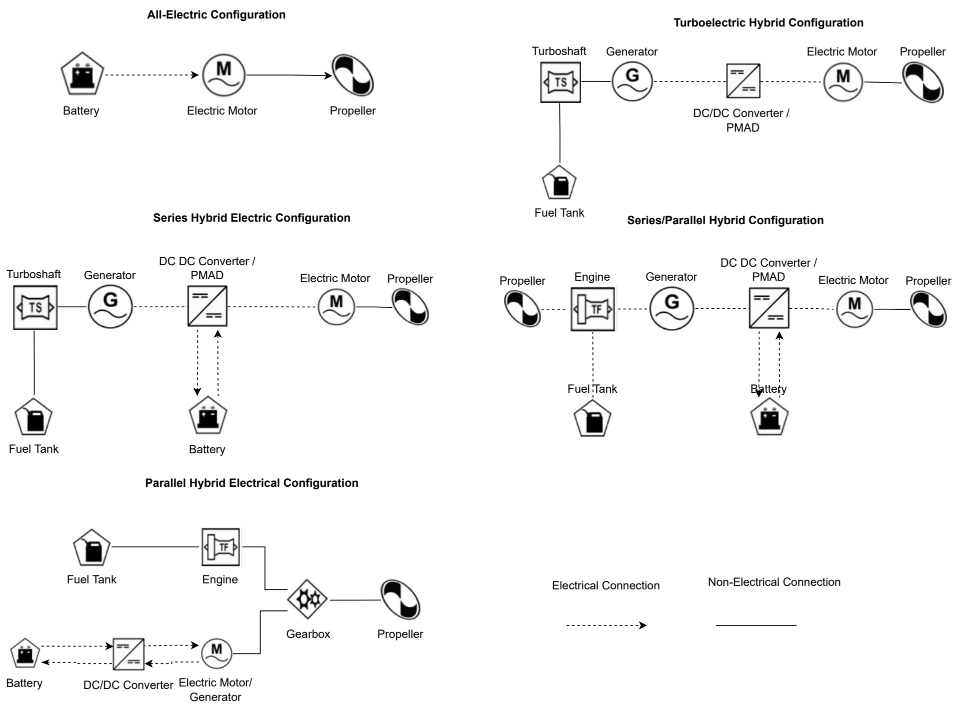

FIGURE 2.2: Propulsion Architecture

Series Hybrid Architecture

In a series hybrid architecture for aircraft, the electric motor is directly connected to the propeller and is powered by a combination of the turbine engine and batteries. The internal combustion engine is not connected to the propeller, which allows it to run at optimal conditions and increases fuel efficiency. This configuration also provides flexibility in the placement of the internal combustion engine.

However, there are some downsides to the series hybrid architecture. One major disadvantage is that there are significant power losses in the combustion and electrical energy conversion process, which reduces overall system efficiency. Additionally, the aircraft may require a larger battery capacity to compensate for the power losses, which can be heavy and costly. Furthermore, the complexity of the powertrain and the integration of the turbine engine, electric motor, and the battery can increase maintenance and operational costs **xie_review_2021**.

Turboelectric Architecture

The turboelectric architecture uses the turbine engine to drive a generator that produces electricity which then goes into a converter to drive the electric motors, which eventually drive the propeller. The turboelectric architecture uses purely the turbine engine to generate electricity, which means that it only uses fuel as energy storage and converts it to electricity **zhang_sustainable_2022**.

Series/Parallel Hybrid Architecture

The series-parallel architecture is a hybrid architecture that merges parallel and series configuration designs. In this configuration, as shown in Figure 2.2, components such as the propeller, internal combustion engine (ICE), electric motor, and generator are all linked to a planetary gear. This architecture facilitates power distribution and allows the ICE and electric motor to operate at their most efficient levels. Despite being the most advanced hybrid propulsion system, the series-parallel architecture requires a complex mechanical coupling mechanism and energy management **xie_review_2021**.

Parallel Hybrid Architecture

In parallel hybrid architecture, the conventional internal combustion engine and the electric motor work together to provide power to the airplane, thus benefiting both systems. The advantage of this system is that it allows both ICE and electric motors to operate more efficiently compared to traditional ICE-only systems and allows the use of a smaller and lighter ICE, as the electric motor can provide additional power. Also, the ICE can simultaneously drive the propeller and the motor/generator can either drive the propeller or charge the battery pack **xie_review_2021**.

2.2 Hybrid-electric Power Management

Power management in hybrid-electric aircraft is essential. It is responsible for the reasonable distribution from both energy sources (i.e battery and fuel) during the flight of the airplane, which directly impacts the efficiency, dynamic, and economy **fang_online_2022**. There has been many research on the power management/energy management of hybrid-electrical aircraft, name a few from Xie et al. **xie_review_2021** and from Voskujil et al. **voskuijl_analysis_2018**.

In Xie's paper **xie_review_2021**, the controller for a hybrid-electrical propulsion system (HEPS) is different from the conventional non-hybrid vehicle's controller. HEPS generally recognize the controller as having two levels; (1) Supervisory Control and (2) Component Control. The supervisory controller performs at the energy management level, dividing power or torque requests between the electric motor and internal combustion engines. The lower-level component controller got issued command by the supervisory controller, which controls the operation of each subsystem (component). The need for energy management has increased interest in and has many research into the study of supervisory control. There are two types of energy management strategies for hybrid propulsion systems; causal and non-causal. The main distinction between those two management strategies is their objective. The causal approach focuses on the optimization at a single node, whereas the non-causal one aims to optimize performance throughout the entire mission.

In Voskujil's paper **voskuijl_analysis_2018**, the strategy management is similar to supervisory control, which divides the power request from the two engines. In his paper, two strategies are investigated: (1) Constant power split and (2) Constant operating mode of the gas turbine. The power setting (throttle) ratio between the electric motor and gas turbine is fixed in a constant power split. Whereas in the second strategy, the gas turbine input is predetermined, and it operates at peak efficiency throughout the majority of the mission. The electric motor provides the remaining power for the mission. Figure 2.3 shows the mission simulation example using the constant power split strategy.

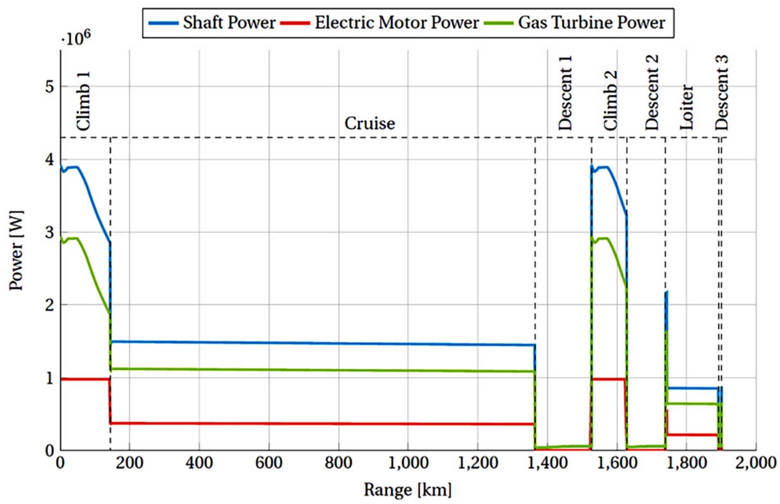

FIGURE 2.3: Mission Simulation example for constant power split with extended range for diversion to alternate airport **voskuijl_analysis_2018**

2.3 Current and future battery technology

One of the essential technologies to support the hybrid-electric propulsion system for airplanes, particularly in bigger aircraft, is energy storage. The current technology for batteries is; alkaline, lead-acid, nickel-cadmium (Ni-Cd), nickel metal hydride (Ni-MH), lithium-ion (Li-ion), and lithium-ion polymer (Li-pol) **rendon_aircraft_2021**. The latter two battery technologies are the most available currently.

Currently, Lithium-ion (Li-ion) batteries with a specific energy of around 250 Wh/kg are commercially available for automotive applications. There are claims that it is possible to achieve 400 Wh/kg with silicon or silicon-carbon anodes and a high-Ni NMC Cathode. Despite the claims that silicon or silicon-carbon anodes can achieve 400 Wh/kg at the cell level, the cell-specific energy of silicon-based anodes for long-life applications will likely be on the order of 350 Wh/kg. Li-metal is the optimal anode for achieving cell-level specific energy greater than 400 Wh/kg. Options for cathodes comprise high-Ni NMC and sulfur **misra_energy_2018**.

Another battery technology, lithium-air, has a theoretical BED that is anywhere from five to ten times higher compared to Lithium-ion. These batteries consist of lithium anode and cathode that is called "air" that is made of a porous material that can absorb oxygen **rajashekara_parallel_2014 rendon_aircraft_2021**. Another type of Li-air battery is an aqueous Li-air battery. The battery could bear, theoretically, a battery energy density of more than 1700 Wh/kg, and it does not have the critical pure oxygen atmosphere, which is an issue for the non-aqueous Li-air battery system, which is more promising for the real-world application **chen_recent_2022**.

NASA recently made progress on its development, making the solid-state battery called Solid-state Architecture Batteries for Enhanced Rechargeability and Safety (SABERS). The materials they are using are primarily sulfur and selenium. In comparison to lithium-ion batteries, these cells can be stacked without the need for separators. So all of the cells in the SABERS battery can be stacked inside a single casing. This battery can power objects at a huge capacity of 500 Wh/kg. This battery also can eliminate 30 to 40 percent of the battery's weight and allows it to double or even triple the energy it can store as compared to the lithium-ion batteries that are considered as the state of the art**gipson_nasas_2022**.

Figure 2.4 shows the assumption and prediction made by Scholz **Scholz_environmental_2022** They surveyed the battery's specific energy as technology forecasts are hard to predict. The survey shows that the battery's specific energy trend is going upward. Though this is not an omnipotent prediction, hopefully, in the future, we will find more and more advancements in battery technologies, and we can achieve the electrification of the aircraft industry.

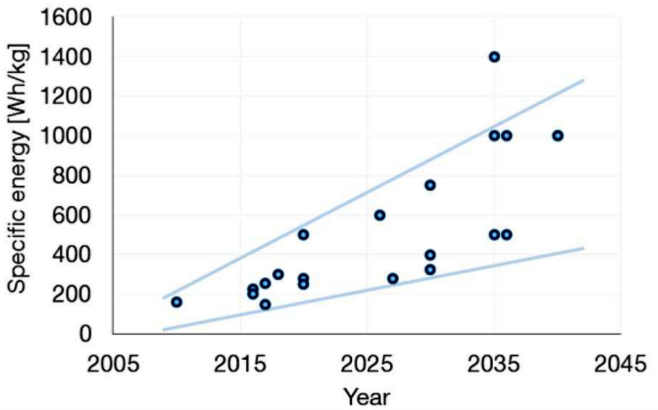

FIGURE 2.4: Asssumed and predicted battery-specific energy in various studies. **Scholz_environmental_2022**

2.4 Equation of Motion

2.4.1 Translational Motion

The forces used to propel an airplane can be correlated with Newton's second law of motion, where the Force of the airplane is equal to the weight of the airplane times the acceleration of the airplane. The forces can be written as

$$\vec{F} = \frac{d(M\vec{V})}{dt} \tag{2.4}$$

Note that in this Equation, the $\vec{F}$ represents the sum of all resultant forces applied on the airplane, and the $\vec{V}$ represents the linear velocity vector of the center of gravity of the body's relative to an inertial reference frame, and M represents the airplane's weight.

In practice, all aircraft structure is flexible, meaning that the relative position of various parts of the structure changes somewhat under the influence of forces acting in flight. However, it is beneficial and justified to ignore these deformations when solving for the motion of an aircraft. Hence, assuming the aircraft is a rigid body with a constant mass, the Equation (2.4) becomes

$$\vec{F} = M\frac{d\vec{V}}{dt} = M\vec{a} \tag{2.5}$$

The translational motion of rigid airplanes of constant mass on Equation 2.5 will be defined using the body axis system. Then the Equation becomes

$$\vec{F} = M\left(\frac{\delta\vec{V}}{\delta t} + \vec{\Omega}\times\vec{V}\right) \tag{2.6}$$

Where the $\frac{\delta\vec{V}}{\delta t}$ represent the derivative of velocity factor with respect to the body axis system, and $\vec{\Omega}$ represent as the angular velocity of the airplane.

2.4.2 Special Types of Flight

In special types of flight there are several kinds, namely;

1. Steady straight non-sideslipping flight;
2. Steady straight sideslipping flight;
3. Flat turn;
4. Steady non-sideslipping banked turn.

But in this thesis, we only discuss the steady straight non-sideslipping flight as this is the only state of flight that will be used.

Steady Straight Non-sideslipping Flight

In this particular state of flight, the lateral variables are zero ($\beta = 0$, C = 0, S = 0, and $\mu = 0$), thus the forces acting on the airplane can be made into

$$\left.\begin{aligned} -D + T\cos\alpha_T - W\sin\gamma = 0 \\ -L - T\sin\alpha_T + W\cos\gamma = 0 \end{aligned}\right\} \tag{2.7}$$

In addition, to achieve balanced moments, the aerodynamic forces must generate forces that can be balanced by proper adjustments of control surfaces where (trimmed flight condition Mx, My, and Mz equal zero). The use of control surfaces affects the aircraft's aerodynamic characteristics, but for this special type of flight, it is assumed that the influence of control surface deflection on the lift, drag, and the side force is minimal in magnitude, and thus can be neglected. Additionally, Our focus is primarily on the airplane's translational motion, thus we can limit ourselves to the force Equations only.

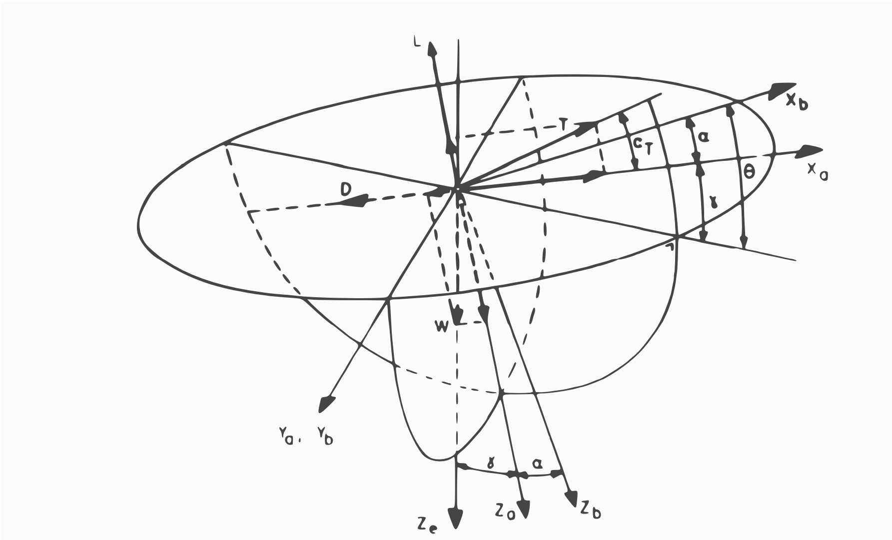

FIGURE 2.5: Steady Straight Non-sideslipping flight

2.5 Aerodynamics Basics

2.5.1 Parabolic lift drag polar

The total drag of an airplane can be split into two categories the component drag (D_n) and the drag of the wing (D_w), then we can write the sum of the total drag for an airplane as

$$D = D_w + D_n \tag{2.8}$$

Then we know that the wing drag is the summation of profile drag and induced drag, thus Equation 2.8 can be modified into,

$$D = D_i + D_p + D_n \tag{2.9}$$

Induce drag is the drag that caused by the lift force, so as the lift force increases the drag force also corresponds with it. Profile drag, which includes pressure drag, skin friction drag, and wave drag is the drag produced from the separation of the

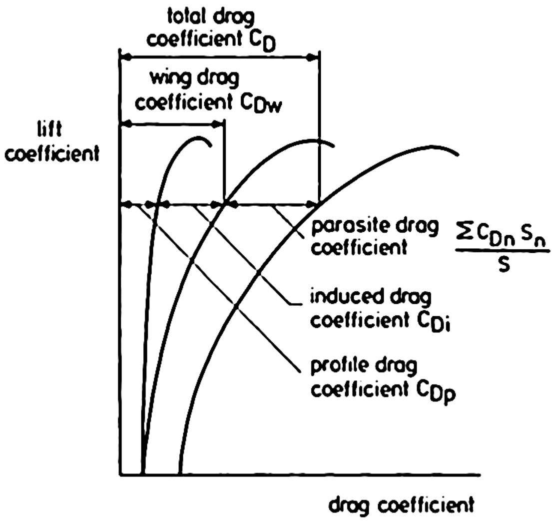

FIGURE 2.6: components of drag coefficient **ruijgrok_elements_2009**

boundary layer from a surface, frictional shear stress on the surface, and the wave from the separation **anderson_aircraft_1998**. The wave drag is only present if the airplane speed is above the subsonic region (M>1), otherwise the wave drag component will be absent. The component drag is also a result of the combination of pressure drag, skin friction drag, and wave drag. Since the drag coefficient of each component of the airplane is based on a certain area as the reference, the Equation of the total drag will be

$$C_D \frac{1}{2}\rho V^2 S = C_{Di}\frac{1}{2}\rho V^2 S + C_{Dp}\frac{1}{2}\rho V^2 S + \left(\Sigma C_{Dn} S_n\right)\frac{1}{2}\rho V^2. \tag{2.10}$$

Then we can eliminate the common variable from both sides, and then the drag coefficient can be rewritten as

$$C_D = C_{Di} + C_{Dp} + \frac{\Sigma C_{Dn} S_n}{S}, \tag{2.11}$$

Where the $\frac{\Sigma C_{Dn} S_n}{S}$ is the parasite drag coefficient.

The generated induced drag coefficient is predicted by theoretical aerodynamics to be directly proportional to the square of the lift coefficient (C_L) and inversely proportional to the aspect ratio (AR) and wing efficiency factor (ϕ). The factor ϕ

principally depends on the wing planform because it shows how closely the elliptic spanwise lift distribution is produced. When the lift distribution is elliptic, the factor ϕ will be equal to 1 (minimum induce drag coefficient), and K will be less than one in all other circumstances. The induced drag coefficient will be

$$C_{Di} = \frac{C_L^2}{\pi A \phi} \tag{2.12}$$

Then substitute Equation 2.12 to Equation 2.11, and the Equation of the drag coefficient of the airplane will be

$$C_D = \frac{C_L^2}{\pi A \phi} + C_{Dp} + \frac{\Sigma C_{Dn} S_n}{S} \tag{2.13}$$

Because the profile drag and parasite drag coefficients are also affected by the angle of attack, the Equation of the drag coefficient will be

$$C_D = \frac{C_L^2}{\pi A \phi} + X C_L^2 + \left[C_{Dp} + \frac{\Sigma C_{Dn} S_n}{S} \right]_{C_L=0} \tag{2.14}$$

Inside the parentheses is termed as the zero-lift drag coefficient (C_{D0}) and the XC_L^2 represent the assumed parabolic change of the profile and parasite drag coefficient with lift coefficient, thus the Equation can be rewritten as

$$C_D = C_{Do} + \frac{C_L^2}{\pi A R e} \tag{2.15}$$

Where the e in the equation is called Oswald's efficiency factor, the Equation as follows

$$\frac{1}{e} = X \pi A + \frac{1}{\phi} \tag{2.16}$$

This factor accounts for the profile and parasite drag coefficient variation with lift coefficient and the impact on the actual spanwise lift distribution on the induced drag coefficient. This factor's value for most airplane types varies between 0.6 and 0.9.

In some circumstances, the induced drag factor or K factor, which can be calculated as $1/ARe$, can be applied to simplify Equation 2.15 as

$$C_D = C_{Do} + k C_L^2 \tag{2.17}$$

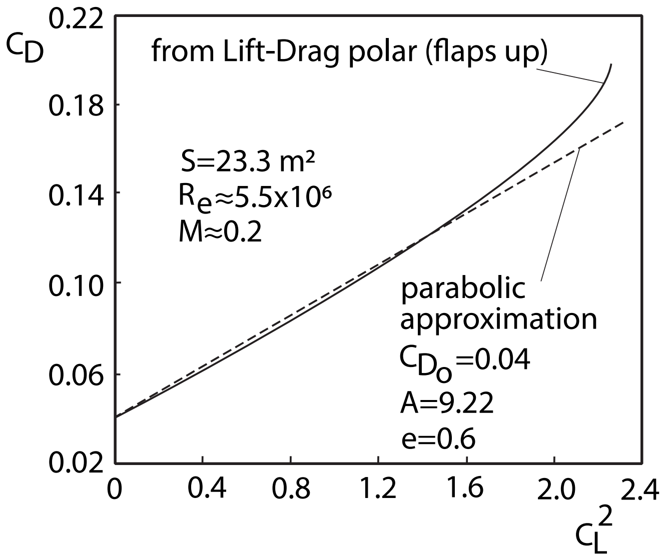

FIGURE 2.7: parabolic approximation of lift-drag polar of low-subsonic airplane

From Figure 2.7, the divergence from the straight (dotted) line illustrates the deviation from the parabolic form, and we can see that a sizeable portion of the lift-drag polar is in fact a parabola, although there is some additional drag at lift coefficient about 1.0 and above.

Suppose the value of C_{Do} and K in Equation 2.17 are modified appropriately. In that case, the parabolic lift-drag polar can be used not only at subsonic speeds but also at transonic and supersonic airspeeds. It should be noted that the following aerodynamic ratios dictate the airplane performance in numerous ways, which are the C_L/C_D, C_L^3/C_D^2, and C_L/C_D^2. And the maximum values of these ratios are important.

To find the maximum value of C_L/C_D, we first differentiate this ratio with respect to C_L and set the Equation to zero.

$$
\begin{aligned}
&\frac{d\left(C_L/C_D\right)}{dC_L} = 0 \\
&\frac{\frac{dC_D}{dC_L}C_D - C_L\frac{dC_D}{dC_L}}{C_D^2} = 0 \\
&C_D - C_L\frac{dC_D}{dC_L} = 0 \\
&C_D = C_L\frac{dC_D}{dC_L} \\
&\frac{dC_D}{dC_L} = \frac{C_D}{C_L}
\end{aligned}
\tag{2.18}
$$

Where,

$$
\begin{aligned}
C_D &= C_{Do} + \frac{\left(\sqrt{\pi AReC_{Do}}\right)^2}{\pi ARe} \\
C_D &= C_{Do} + C_{Do} \\
C_D &= 2C_{Do}
\end{aligned}
\tag{2.19}
$$

Then substitute Equation 2.19 to Equation 2.18, then we can obtain C_L as

$$
\begin{aligned}
\frac{C_D}{C_L} &= \frac{2C_L}{\pi ARe} \\
2C_L^2 &= \pi A\,\mathrm{Ae}\,C_D \\
2C_L^2 &= \pi A\,\mathrm{Re}\left(C_{Do} + \frac{CL^2}{\pi ARe}\right) \\
2C_L^2 &= \pi A\,\mathrm{Ae}\,C_{Do} + C_L^2 \\
C_L^2 &= \pi A\,\mathrm{Re}\,C_{Do} \\
C_L &= \sqrt{\pi A\,\mathrm{Ae}\,C_{Do}}
\end{aligned}
\tag{2.20}
$$

Substituting the C_L and C_D that we have obtained before, we can find the $(C_L/C_D)_{max}$ as

$$
\begin{aligned}
\left(\frac{C_L}{C_D}\right)_{max} &= \frac{CL}{CD} \\
&= \frac{\sqrt{\pi AReC_{DO}}}{2C_{DO}}
\end{aligned}
\tag{2.21}
$$

$$\left(\frac{C_L}{C_D}\right)_{\max} = \frac{1}{2}\sqrt{\frac{\pi ARe}{C_{Do}}} \tag{2.22}$$

For finding the C_L^3/C_D^2 we can use the similar approach as we find the $(C_L/C_D)_{max}$ as follows

$$\frac{dC_D}{dC_L} = \frac{C_D^3}{C_L^2} \tag{2.23}$$

the we find the C_L and C_D for the condition,

$$\frac{2C_L}{\pi Ae} = \frac{3}{2}\left[\frac{C_{D_0} + C_L^2/(\pi ARe)}{C_L}\right] \text{ or } C_L = \sqrt{3C_{D_0}\pi Ae} \tag{2.24}$$

$$C_D = 4C_{D_0} \tag{2.25}$$

then we can substitute the C_L and C_D to Equation 2.23

$$\left(\frac{C_L^3}{C_D^2}\right)_{\max} = \frac{3C_{D_0}\pi \cdot ARe\sqrt{3C_{D_0}\pi Ae}}{16C_{D_0}^2} \tag{2.26}$$

Then the final equation is as follows

$$\left(\frac{C_L^3}{C_D^2}\right)_{\max} = \frac{3\sqrt{3}}{16}\pi ARe\sqrt{\frac{\pi ARe}{C_{Do}}} \tag{2.27}$$

For C_L/C_D^2 with the same approach as both ratios before,

$$\frac{dC_D}{dC_L} = \frac{C_D}{C_L^2} \tag{2.28}$$

the we find the C_L and C_D for the condition,

$$C_L = \sqrt{\frac{1}{3}C_{D_0}\pi ARe}, \tag{2.29}$$

$$C_D = \frac{4}{3}C_{D}o \tag{2.30}$$

then we can substitute the C_L and C_D to Equation 2.28

$$\left(\frac{C_L}{C_D^2}\right)_{\max} = \frac{3\sqrt{3}}{16}\sqrt{\frac{\pi ARe}{C_{D_0}^3}} \tag{2.31}$$

2.6 Range Performance

2.6.1 Range

The term range according to Ruijgrok is used for the horizontal straight-line distance of an aircraft during cruising flight as shown in Figure 2.8. On the other hand, for the climb, cruise, and descent, the distance would be called total range, stage length, or block distance **ruijgrok_elements_2009**.

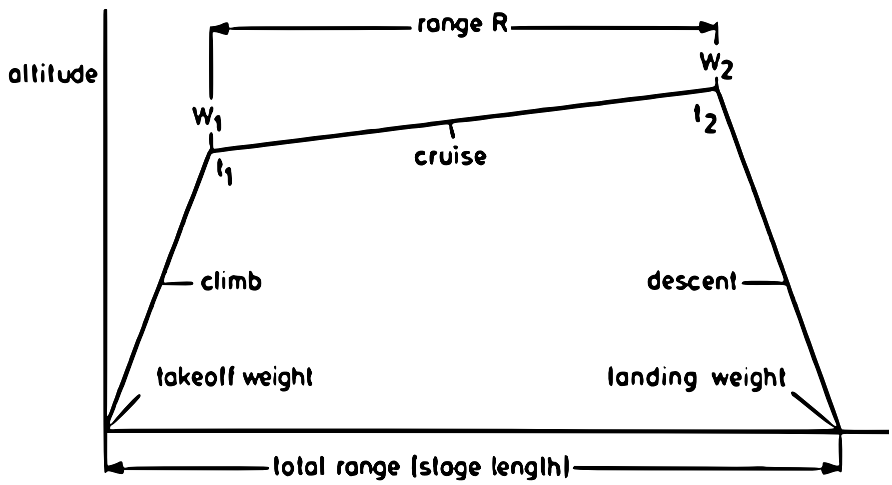

FIGURE 2.8: Mission Nomenclature

To get the maximum total range of an aircraft, we should calculate the fuel consumption per unit of time because the maximum total range is defined as the distance an aircraft can fly between takeoff and landing limited by the fuel capacity.

$$F = \frac{dW_{\text{fuel}}}{dt} \tag{2.32}$$

note that W_{fuel} is the total fuel load, and since the fuel weight flow is related to the weight of the aircraft $dW_{\text{fuel}} = -dW$, thus the Equation 2.32 can be rewritten as:

$$F = -\frac{dW}{dt} \tag{2.33}$$

From the following integral Equation, we could acquire the range as

$$R = \int_{t_1}^{t_2} V dt = \int_{W_1}^{W_2} -\frac{V}{F} dW = \int_{W_2}^{W_1} \frac{V}{F} dW \tag{2.34}$$

where the $\frac{V}{F}$ is the specific range in which the range per unit weight of fuel and the subscript of "1" is defined as the initial condition and the subscript of "2" is the final condition of the cruise.

In symmetric flight, it is important to remember that the time history of the flight condition depends on the specification of the two control law, pitch control law and engine control law, and the description of the variation of those two control law variables with the time. Generally, both control variables are held constant throughout the cruise so that the flight condition only changes due to the influence of fuel consumption on airplane weight **ruijgrok_elements_2009**.

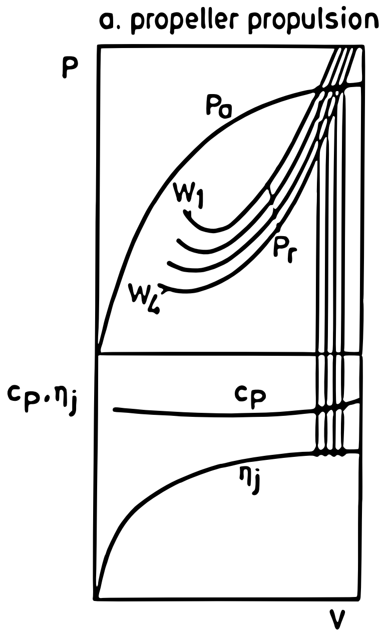

FIGURE 2.9: Determination of V/F and F during flight at a constant altitude and engine control setting

Figure 2.9 illustrated the procedure of determining the F and V/F as a function of airplane weight for a propeller-driven airplane with the assumption of it performed on a level flight and constant engine control. For propeller-driven propulsion, the computation needs to be at the equilibrium condition where the power available (P_a) is equal to the power required (P_r), and there corresponds to a particular value of propulsive efficiency (η_j) and specific fuel consumption (C_P).

$$\begin{aligned} \eta_j &= \frac{P_a}{P_{br}} \\ P_{br} &= \frac{P_a}{\eta_j} \end{aligned} \tag{2.35}$$

And for the corresponding fuel weight flow can be calculated by using the following Equation.

$$\begin{aligned} F &= C_P P_{br} \\ F &= C_P \frac{P_a}{\eta_j} \end{aligned} \tag{2.36}$$

Figure 2.9 illustrates the range from plotting V/F against W.

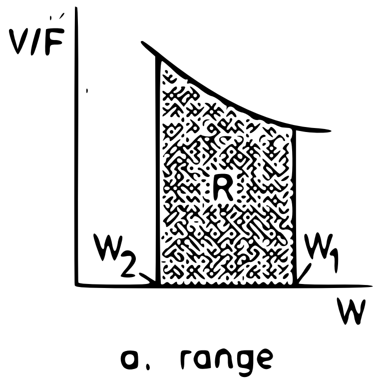

FIGURE 2.10: Range calculation

2.6.2 Approximate Analytic Expression for Range (Conventional Turboprop Aircraft)

To obtain the analytical expression for range, we can use Equation 2.35 and 2.36, then we can write it as

$$F = c_p P_{br} = c_p \frac{P_a}{\eta_j} = c_p \frac{P_r}{\eta_j} = c_p \frac{DV}{\eta_j}. \tag{2.37}$$

Using the relation of velocity (V) and drag (D)

$$V = \sqrt{\frac{W}{S} \frac{2}{\rho} \frac{1}{C_L}} \tag{2.38}$$

$$D = \frac{C_D}{C_L} W \tag{2.39}$$

We can obtain

$$\frac{V}{F} = \frac{\eta_j}{c_p} \frac{C_L}{C_D} \frac{1}{W} \tag{2.40}$$

$$F = \frac{c_p}{\eta_j} W \sqrt{\frac{W}{S} \frac{2}{\rho} \frac{C_D^2}{C_L^3}} \tag{2.41}$$

Then by substituting Equation 2.40 into 2.34 we can get

$$R = \int_{W_1}^{W_2} \frac{\eta_j}{c_p} \frac{C_L}{C_D} \frac{dW}{W} \tag{2.42}$$

Analyzing Equation 2.42 shows that from an analytical perspective, it's intriguing

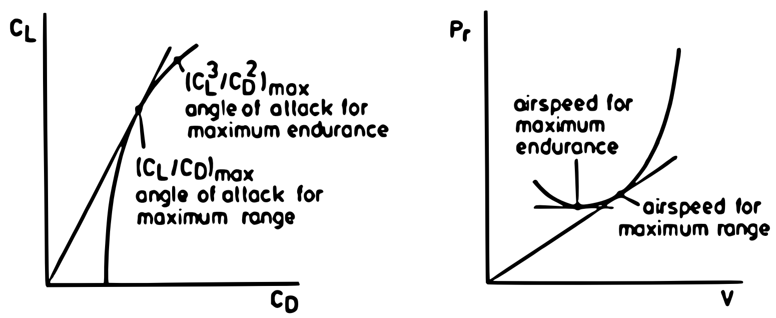

FIGURE 2.11: Best range condition in level flight for propeller-driven airplane

to consider the cruise method where the angle of attack stays the same throughout the flight. Additionally, the variables η_j and C_P tend only to have minimal fluctuation over the range of cruising speeds, making it reasonable to assume they have steady average values. Then the Equation 2.42 can be integrated to give an approximation of range,

$$R = \frac{\eta_j}{c_p}\frac{C_L}{C_D}\int_{W_1}^{W_2}\frac{dW}{W} = \int_{W_1}^{W_2}\frac{\eta_j}{c_p}|\ln W|_{W_2}^{W_1} \tag{2.43}$$

Which then can be rewritten known as the classic Breguet formula for range,

$$R = \frac{\eta_j}{gc_p}\frac{C_L}{C_D}ln\left(\frac{W_1}{W_2}\right) \tag{2.44}$$

Figure 2.11 shows the best range and endurance condition in level flight. For the maximum range, the airplane must fly at an angle of attack where the C_L/C_D is the maximum.

2.6.3 Approximation Analytic Expression for Range (Hybrid Electric Aircraft)

voskuijl_analysis_2018, **voskuijl_correction_2020** For a conventional fuel-powered aircraft, the range can be calculated using the Breguet range equation:

$$R = \int_{W_{\text{start}}}^{W_{\text{finish}}}\frac{V}{C_t}\frac{C_L}{C_D}\frac{1}{W}dW \tag{2.45}$$

But the Equation cannot be applied to an aircraft that partially uses the battery as the energy supply since the batteries have a constant weight during the flight and the Breguet range Equation was based on weight reduction (fuel). Fundamentally, the range can be determined by integrating speed over time.

$$R = \int_{t_{\text{start}}}^{t_{\text{final}}} V dt \tag{2.46}$$

For the hybrid-electric Equation, we can solve it using the energy reduction over time, since the energy stored in the batteries or fuel reduces.

$$\frac{dE}{dt} = \frac{dE_{\text{fuel}}}{dt} + \frac{dE_{\text{bat}}}{dt} \tag{2.47}$$

and by substitute the Equation 2.47 to 2.46 we get

$$R = \int_{E_{\text{start}}}^{E_{\text{final}}} \frac{V}{\frac{dE_{\text{fuel}}}{dt} + \frac{dE_{\text{bat}}}{dt}} dE \tag{2.48}$$

Then there is a hybridization factor (ψ) (energy degree of hybridization), which are the ratio of the energy (E) stored in the battery with the total energy in both fuel and batteries.

$$\psi = \frac{E_{\text{bat}}}{E_{\text{total}}} = \frac{E_{\text{bat}}}{E_{\text{fuel}} + E_{\text{bat}}} \tag{2.49}$$

Power split:

$$H_{\text{P}} = \frac{P_{\text{em}}}{P_{\text{total}}} = \frac{P_{\text{em}}}{P_{\text{em}+P_{\text{ICE}}}} \tag{2.50}$$

and the supply power ratio is the ratio of powers integrated over the full block flight mission

$$\Phi = \frac{\int_{t=0}^{t_{bt}} P_{em}(t)dt}{\int_{t=0}^{t_{bt}} P_{\text{total}}(t)dt} \tag{2.51}$$

for the fuel energy

$$F = -\frac{W_{\text{fuel}}}{dt} = -\frac{g}{H_{\text{fuel}}}\frac{dE_{\text{fuel}}}{dt} \tag{2.52}$$

then

$$F = C_p P_{\text{br, gasturbine}} \tag{2.53}$$

where Pr Gas Turbine

$$\begin{aligned} P_{\text{br, gasturbine}} &= (1-S)P_{\text{br,total}} \\ &= (1-S)\frac{P_{\text{a}}}{\eta_{\text{prop}}} \end{aligned} \tag{2.54}$$

For the energy derivation of battery and fuel:

$$\frac{dE_{\text{fuel}}}{dt} = -\frac{cE}{\eta_{\text{prop}}}\frac{H_{\text{fuel}}}{g}(1-S)P_{\text{a}} \tag{2.55}$$

$$\frac{dE_{\text{bat}}}{dt} = -\frac{P_{\text{br,electric}}}{\eta_{\text{electric}}} = -\frac{S}{\eta_{\text{electric}}\eta_{\text{prop}}} P_{\text{a}} \tag{2.56}$$

Substitute Equation 2.55 and 2.56 to Equation 2.47

$$\frac{dE_{\text{total}}}{dt} = \left(\frac{cE}{\eta_{\text{prop}}} \frac{H_{\text{fuel}}}{g} + \frac{S}{\eta_{\text{electric}}\eta_{\text{prop}}} \right) P_{\text{a}} \tag{2.57}$$

Then find the Power Available (P_{a})

$$P_{\text{a}} = D \cdot V = \frac{C_D}{C_L} W \cdot V \tag{2.58}$$

Insert the power available to dE_{total}.

$$\frac{dE_{\text{total}}}{dt} = \left(\frac{c_p}{\eta_{\text{prop}}} \frac{H_{\text{fuel}}}{g} (1-S) + \frac{S}{\eta_{\text{electric}}\eta_{\text{prop}}} \right) \frac{C_D}{C_L} W V \tag{2.59}$$

Searching for V:

$$V = \frac{1}{\left(\frac{c_p}{\eta_{\text{prop}}} \frac{H_{\text{fuel}}}{g} (1-S) + \frac{S}{\eta_{\text{electric}}\eta_{\text{prop}}} \right) \frac{C_D}{C_L} W} \frac{dE_{\text{total}}}{dt} \tag{2.60}$$

From then the range equation for a hybrid-electric can be found by combining the Equation 2.60 and 2.46

$$R = \int_{E_{\text{start}}}^{E_{\text{final}}} \frac{1}{\left(\frac{c_p}{\eta_{\text{prop}}} \frac{H_{\text{fuel}}}{g} (1-S) + \frac{S}{\eta_{\text{electric}}\eta_{\text{prop}}} \right)} \frac{C_L}{C_D} \frac{1}{W} dE \tag{2.61}$$

With the assumption that all other than the weight is constant throughout the mission.

$$R = \frac{1}{\left(\frac{c_p}{\eta_{\text{prop}}} \frac{H_{\text{fuel}}}{g} (1-S) + \frac{S}{\eta_{\text{electric}}\eta_{\text{prop}}} \right)} \frac{C_L}{C_D} \int_{E_{\text{start}}}^{E_{\text{final}}} \frac{1}{W} dE \tag{2.62}$$

Weight distribution

$$W = W_{empty} + W_{\text{payload}} + W_{\text{battery}} + W_{\text{fuel}} \tag{2.63}$$

$$W = \frac{E_{\text{bat}}}{H_{\text{bat}}} g + \frac{E_{Fuel}}{H_{\text{fuel}}} g + W_{\text{payload}} + W_{empty} \tag{2.64}$$

Using the hybridization factor, the Equation will be.

$$W = \frac{\psi}{H_{\text{bat}}} g E_{\text{start}} + \frac{(1-\psi)}{H_{\text{fuel}}} g E + W_{\text{payload}} + W_{empty} \tag{2.65}$$

Insert the weight into the range Equation.

$$\begin{aligned} R = & \frac{1}{\left(\frac{c_p}{\eta_{\text{prop}}} \frac{H_{\text{fuel}}}{g} (1-S) + \frac{S}{\eta_{\text{electric}} \eta_{\text{prop}}} \right)} \frac{C_L}{C_D} \\ & \int_{E_{\text{start}}}^{E_{\text{final}}} \frac{1}{\frac{\psi}{H_{\text{bat}}} g E_{\text{start}} + \frac{(1-\psi)}{H_{\text{fuel}}} g E + W_{\text{payload}} + W_{empty}} dE \end{aligned} \tag{2.66}$$

Solving the integral of the energy.

$$W = \frac{\psi}{H_{\text{bat}}} g E_{\text{start}} + \frac{(1-\psi)}{H_{\text{fuel}}} g E + W_{\text{payload}} + W_{empty} \tag{2.67}$$

derive the weight with respect to the energy (E)

$$\frac{dW}{dE} = \frac{(1-\psi)}{H_{\text{fuel}}} (g) \tag{2.68}$$

$$dE = \frac{dW}{\frac{(1-\psi)}{H_{\text{fuel}}} (g)} \tag{2.69}$$

Insert dE into the Equation

$$\int_{W_{\text{start}}}^{W_{\text{final}}} \frac{1}{\frac{\psi}{H_{\text{bat}}} g E_{\text{start}} + \frac{(1-\psi)}{H_{\text{fuel}}} g E + W_{\text{payload}} + W_{empty}} \frac{dW}{\frac{(1-\psi)}{H_{\text{fuel}}} g} \tag{2.70}$$

Set:

$$W_{\text{fuel}} \text{ as } \frac{(1-\psi)}{H_{\text{fuel}}}(g)$$
$$W \text{ as } \frac{\psi}{H_{\text{bat}}} g E_{\text{start}} + \frac{(1-\psi)}{H_{\text{fuel}}} g E + W_{\text{payload}} + W_{empty}$$

Then

$$\int_{W_{\text{start}}}^{W_{\text{final}}} \frac{1}{W} \frac{dW}{W_{\text{fuel}}} \tag{2.71}$$

$$\frac{1}{W_{\text{fuel}}} \int_{W_{\text{start}}}^{W_{\text{final}}} \frac{1}{W} dW \tag{2.72}$$

$$W_{\text{fuel}} \left[ln|W_{\text{start}}| - ln|W_{\text{finish}}| \right] \tag{2.73}$$

with the laws of logarithmic

$$W_{\text{fuel}} \left[ln \frac{|W_{\text{start}}|}{|W_{\text{finish}}|} \right] \tag{2.74}$$

by inserting the weight, the range hybrid electric can be written:

$$R_{hybrid} = \frac{1}{\left(\frac{c_p}{\eta_{\text{prop}}} \frac{H_{\text{fuel}}}{g}(1-S) + \frac{S}{\eta_{\text{electric}}\eta_{\text{prop}}} \right)} \frac{C_L}{C_D} \frac{H_{\text{fuel}}}{g} \frac{1}{(1-S)} \left(\frac{\frac{\psi}{H_{\text{bat}}} g E_{\text{start}} + \frac{(1-\psi)}{H_{\text{fuel}}} g E + W_{\text{payload}} + W_{empty}}{\frac{\psi}{H_{\text{bat}}} g E_{\text{start}} + W_{\text{payload}} + W_{empty}} \right) \tag{2.75}$$

$$R_{hybrid} = \frac{\eta_{\text{prop}}}{\left(c_p \frac{H_{\text{fuel}}}{g}(1-S) + \frac{S}{\eta_{\text{electric}}} \right)} \frac{C_L}{C_D} \frac{H_{\text{fuel}}}{g} \frac{1}{(1-\psi)} \left(\frac{\frac{\psi}{H_{\text{bat}}} g E_{\text{start}} + \frac{(1-\psi)}{H_{\text{fuel}}} g E + W_{\text{payload}} + W_{empty}}{\frac{\psi}{H_{\text{bat}}} g E_{\text{start}} + W_{\text{payload}} + W_{empty}} \right) \tag{2.76}$$

2.7 Hybrid Electric Battery Estimation

For battery estimation in this thesis, we will be using the Hybridization energy in relation to the total of the reference aircraft fuel mass to estimate fuel and battery mass.

from energy hybridization (ψ)

$$\psi = \frac{E_{\text{bat}}}{E_{\text{total}}} \tag{2.77}$$

$$\psi = \frac{E_{\text{bat}}}{E_{\text{bat}} + E_{\text{fuel}}} \tag{2.78}$$

which E_{bat} is the energy of the battery or for the electric motors and E_{total} is the total energy of the system

$$E_{\text{bat}} = m_{\text{bat}} \times H_{\text{bat}} \tag{2.79}$$

$$E_{\text{fuel}} = m_{\text{fuel}} \times H_{\text{fuel}} \tag{2.80}$$

For the total energy mass in this case is the total fuel/energy mass which can be represented as

$$m_{tot} = m_{\text{fuel}} + m_{\text{bat}} \tag{2.81}$$

now we can substitute Equations 2.79, 2.80, and 2.81 to 2.78

$$\psi = \frac{m_{\text{bat}} \cdot H_{\text{bat}}}{m_{\text{bat}} \cdot H_{\text{bat}} + ((m_{tot} - m_{\text{bat}})\, H_{\text{fuel}})} \tag{2.82}$$

$$m_{\text{bat}} \cdot H_{\text{bat}} = \psi\,(m_{\text{bat}} \cdot H_{\text{bat}} + (m_{tot} - m_{\text{bat}})H_{\text{fuel}}) \tag{2.83}$$

$$m_{\text{bat}} \cdot H_{\text{bat}} = \psi\,(m_{\text{bat}} \cdot H_{\text{bat}} + m_{tot} \cdot H_{\text{fuel}} - m_{\text{bat}} \cdot H_{\text{fuel}}) \tag{2.84}$$

$$\frac{m_{\text{bat}} \cdot H_{\text{bat}}}{\psi} = m_{\text{bat}}\,(H_{\text{bat}} - H_{\text{fuel}}) + m_{tot} \cdot H_{\text{fuel}} \tag{2.85}$$

$$m_{tot} \cdot H_{\text{fuel}} = \frac{m_{\text{bat}} \cdot H_{\text{bat}}}{\psi} - m_{\text{bat}} \cdot (H_{\text{bat}} - H_{\text{fuel}}) \tag{2.86}$$

$$m_{tot} \cdot H_{\text{fuel}} = \frac{m_{\text{bat}} \cdot H_{\text{bat}}}{\psi} - m_{\text{bat}} \cdot H_{\text{bat}} + m_{\text{bat}} \cdot H_{\text{fuel}} \tag{2.87}$$

$$m_{tot} \cdot H_{\text{fuel}} = m_{\text{bat}} \cdot \left(\frac{H_{\text{bat}}}{\psi} - H_{\text{bat}} + H_{\text{fuel}} \right) \tag{2.88}$$

by rearranging the Equation we can get the Equation for battery mass.

$$m_{\text{bat}} = \frac{m_{tot} \cdot H_{\text{fuel}}}{\frac{H_{\text{bat}}}{\psi} - H_{\text{bat}} + H_{\text{fuel}}} \tag{2.89}$$

for fuel mass, we can substitute the battery mass in Equation 2.89 to the total mass in Equation 2.81

$$m_{\text{fuel}} = \frac{m_{tot} \cdot \left(H_{\text{bat}} - \dfrac{H_{\text{bat}}}{\psi} \right)}{\dfrac{H_{\text{bat}}}{\psi} - H_{\text{bat}} + H_{\text{fuel}}} \tag{2.90}$$

CHAPTER 3
RESEARCH METHODOLOGY

In Chapter 3 we will discuss about the methodology that is being used in this thesis. Figure 3.1 represents the steps taken throughout the entire process of making this thesis.

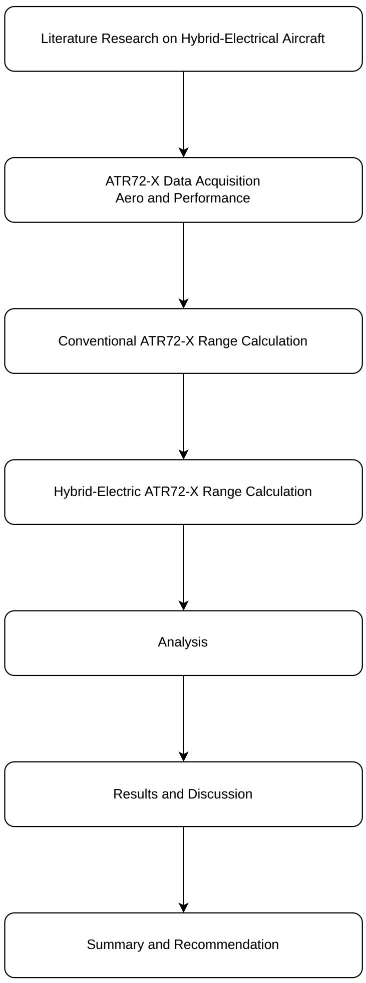

FIGURE 3.1: Research Methodology

The first process is literature research on hybrid-electric aircraft in Chapter 2. The purpose is to know and understand about hybrid-electric aircraft, because hybrid-electric systems themselves have different configurations as explained in literature research in Chapter 2 which in each of its configurations uses different measurement and calculation methods. The second is the data acquisition of ATR72. This section is about the data gathering of the aircraft as it is one of the important data for calculating the hybrid-electric range as well as doing analysis for this thesis. The next process is the calculation of the range of hybrid-electric aircraft. The calculated variables are the hybridization factors and battery-specific energy. The calculation method are using the range equation for hybrid-electric propeller aircraft provided by Voskujil et al. The battery and fuel weight for the hybrid-electrical system will be defined in this process. Then after that will be results and a discussion of the range performance that has been calculated in the previous step.

3.1 ATR72 Data Acquisition

Table 3.1: ATR72 Data **nita_aircraft_2008**

Parameters	SI Unit	Imperial Unit
Maximum take-off weight	23296.272 kg	51359.488 lb
Maximum landing weight	22830.347 kg	50332.3 lb
Maximum payload	6650 kg	14660.74 lb
Maximum usable fuel	3414.398 kg	7527.459 lb
Maximum zero fuel weight	19881.874 kg	43832.029 lb
Cruise Speed	510 km/h	274.378 Knots
Take off distance	1290 m	4232.283 ft
Landing distance	1067 m	3500.656 ft

Finding data on ATR72 was quite hard although the aircraft itself is an old aircraft, finding specific data such as aerodynamics and its performance is an issue itself. The ATR72 websites and brochures are only providing general data on the aircraft and it's insufficient for this thesis. As a result, the author is going to use a modified ATR72 which is a dissertation made by Mihaela Florentina Nita, a Ph.D. student from FZT Hamburg titled "Aircraft Design Studies Based on the ATR72" **nita_aircraft_2008**. The dissertation provides all the data that are going to be used for this thesis which is presented in Table 3.1 and 3.2. The redesign of this aircraft for this thesis will be called the ATR72-X.

TABLE 3.2: ATR72 Geometry **nita_aircraft_2008**

Aircraft Geometry	SI Unit	Imperial Unit
Wing area	62.187 m^2	669.375 ft^2
Wing span	27.32 m	89.632 ft
Wing Aspect Ratio	12	12
Fueslage Length	27.13 m	89 ft
Fuselage Height	7.65 m	25.09 ft
CMAC	2.1368 m	7.01 ft
CG	11.5586 m	37.921 ft
Zero-Lift drag coefficient C_{d0}	0.002704	0.002704
Lift coefficient at cruise $C_{\mathrm{L,cr}}$	0.81	0.81
Horizontal tailpane area	9.701 m^2	104.42 ft^2
Vertical taiplane area	14.085 m^2	151.6 ft^2
Propeller Diameter	3.93 m	12.86 ft

3.1.1 Propeller Efficiency

For propeller aircraft, the efficiency of the propeller is important as it would affect the performance of the aircraft itself. In Nita's dissertation **nita_aircraft_2008**, for estimating the propeller efficiency they are using a diagram as shown in Figure

3.2. According to this Figure, for determining the propeller efficiency, we need to calculate a parameter presented in equation 3.1:

$$\text{Parameter} = \frac{P_{\text{cruise}}}{\rho \times S_{\text{disc}}} \tag{3.1}$$

But then we need to know first the surface of the propeller in order to determine the parameter which can be calculated by using:

$$S = \frac{d_p^2 \times \pi}{4} \tag{3.2}$$

After knowing the parameter we could estimate the value of propeller efficiency in the diagram shown in Figure 3.2

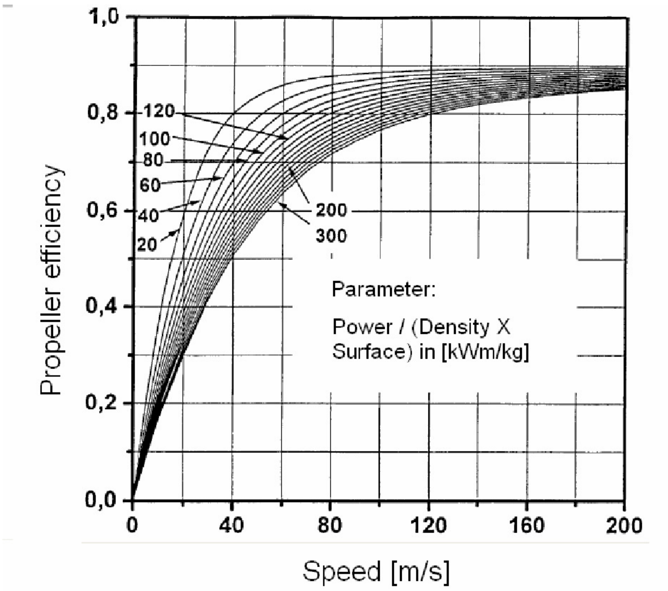

FIGURE 3.2: Propeller Efficiency Diagram

3.1.2 Parabolic Lift-Drag Polar Estimation

In this section, we will be finding the parabolic lift-drag polar for the ATR72-X. The lift, drag, and zero drag coefficients from the aerodynamics profile are utilized as variables to calculate the parabolic lift-drag polar. The calculation will be done by utilizing Equation 2.21, 2.27, and 2.31 respectively to find the values of

- $(C_L/C_D)_{\max}$
- $(C_L^3/C_D^2)_{\max}$
- $(C_L/C_D^2)_{\max}$

3.2 Convetional Range Performance Calculation

Before calculating for hybrid-electrical range, we will calculate the range of the conventional configuration. The calculation will be done by using the Breguet range equation shown in Equation 2.44. Then the results will be for comparing the conventional aircraft range to the hybrid-electrical range.

3.3 Hybrid-Electric Range Performance Calculation

This section discuss how the range performance is being calculated and the steps to calculate as shown in Figure 3.3.

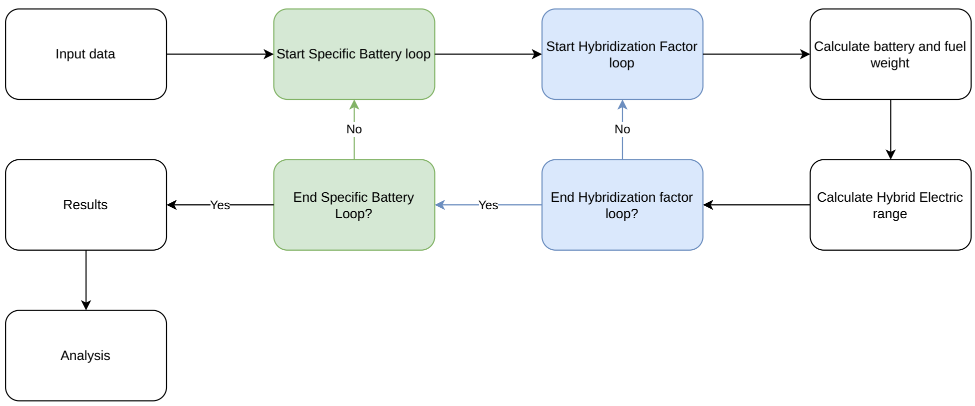

FIGURE 3.3: Performance Calculation Overview

For cruising performance, the flight profile is steady straight flight and the configuration for hybrid-electric is a parallel configuration with constant split power for power management. The following Table are the predefined variable.

TABLE 3.3: hybrid-electric Variable

Parameters	SI Unit	Imperial Unit
Altitude	5100 m	16732.28 ft
Total efficiency	0.903	0.903
Aircraft weight	23296.272 kg	51359.488 lb
Aircraft weight w/o energy sources	19881.874	43832.029 lb
Payload	6650 kg	14660.74 lb
Total weight of energy source	3414.98 kg	7527.459 lb
Zero-lift drag coefficient (C_{D_0})	0.002704	0.002704
Wing aspect ratio (AR)	12	12
C_L/C_D	17.1	17.1

The calculation for the range of the hybrid-electric aircraft is calculated using various specific battery energy ranging from 500 - 1000 Wh/kg and the hybridization power and energy of 0.1 until 0.9 with a step of 0.1. To get the end results, the author first needs to estimate the battery and fuel weight for the aircraft by using Equation 2.89 and Equation 2.90. We need to know the weight of both energy storage to estimate the range of the hybrid systems. Under various hybridization of energy, the battery weight and fuel weight will be different and we want to see how much of a difference under that factor and analyze it. Also, since the battery weight is constant throughout the flight it would be affecting the range performance of the airplane.

Then after knowing both weights of energy storage, we can calculate the range of hybrid-electrical using Equation 2.76. Then the results of the calculation will be analyzed and discussed in Chapter 4 in the form of graphs and more specific results from the calculation will be available in the form of a Table in Appendix 5.3.

CHAPTER 4
RESULTS AND DISCUSSIONS

This Chapter will discuss the result from the calculation and methodology from Chapter 2 and Chapter 3. In section 4.1, we will estimate and analyze the battery and fuel weight of the aircraft without changing the configuration of the aircraft, such as the maximum take-off weight and the fuel mass. Section 4.2 will be discussed the range results of the hybrid electric conversion and how the Hybridization Factors would affect the range performance that can be achieved in these configurations. The full Table for range calculation is available in Appendix A. In section 4.3, We will be comparing the hybrid electric aircraft to the conventional and all-electric according to the calculation method provided in Chapter 2. All calculations for the ATR72-X hybrid will be done assuming the availability of batteries with a specific energy of 500 Wh/kg - 1000 Wh/kg.

4.1 Hybrid Battery and Fuel Weight Estimation

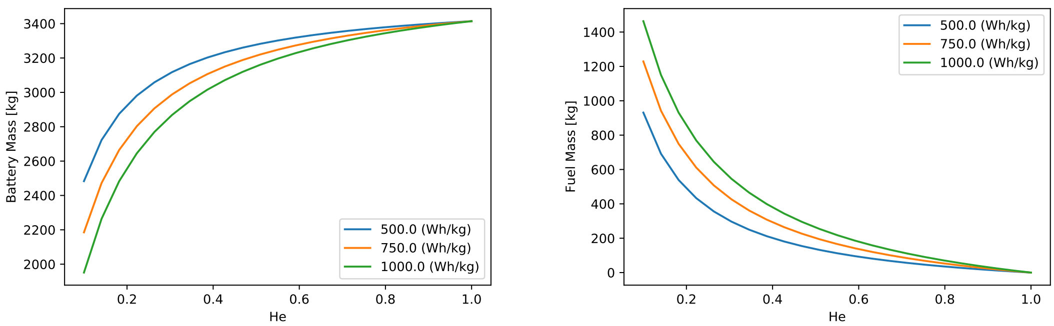

FIGURE 4.1: Battery mass (left) and Fuel mass (right) as a function of Energy Hybridization for various specific battery energy

The effect of the Hybridization of Energy and the specific energy of the battery on the fuel mass and battery mass is investigated using the calculation and methods in the previous Chapters (Figure 4.1). The mass that is going to be used is limited to the MTOW of the reference aircraft without changing any configuration of the aircraft. For the constant MTOW, the effect of energy hybridization (H_E) will result in an increase in battery mass as it goes higher, but on the other hand, the fuel mass will going to be decreased. And if we look at the various battery energy density, the 500 Wh/kg battery has the highest battery mass, and as it goes higher, the battery mass decreases and the fuel mass is the opposite, as the battery density increases the fuel mass will also increase. This result is due being the Energy Hybridization as the ratio of the battery energy to the total overall energy of the system and also searching the maximum total energy from both sources as depicted in Figure 4.2. But ideally, what we want is for as the battery-specific energy increases, the battery mass is also increased, thus lowering the fuel mass and that could lead to lowering the CO2 emission from the aircraft.

Figure 4.2 visualized the total energy of the system as a function of energy hybridization for various battery-specific energy. The higher the specific energy, the higher the total energy in the system but as the energy hybridization increases, the total energy are decreasing. This is due to the changes in battery mass, as the batteries, specific energy is far less than the fuel-specific energy and resulting in lower aircraft range performance that will be discussed later. The results of the total mass, as mentioned earlier, are limited to the maximum fuel mass of the reference aircraft of 3414.98 kg to see if we could convert the aircraft into a hybrid aircraft with the same configuration or without changing the maximum take-off weight of the aircraft and how the energy sources are calculated for the constant MTOW.

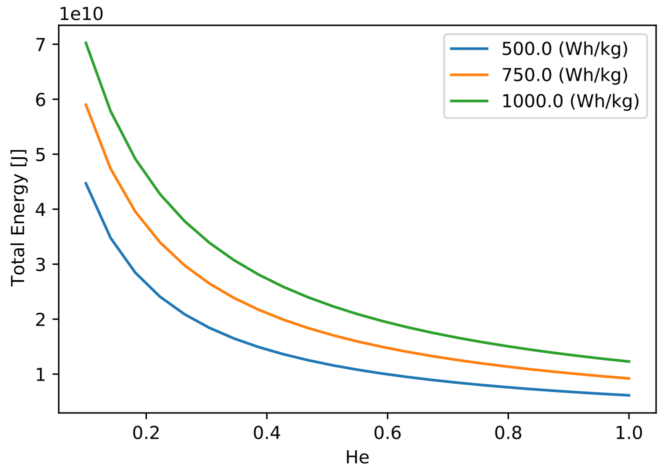

FIGURE 4.2: Total Energy as a function of energy hybridization for various battery-specific energy

4.2 ATR72 Hybrid-electric range

Figure 4.3, 4.4, and 4.5 shows the result of the calculated range of the ATR-72-X Hybrid-Electric Propulsion System (HEPS) over various power split (H_P), Hybridization Energy (H_E), and various battery specific energy starting from the value of 0.1 to 0.9, since H_E and H_P of 0 belongs to conventional aircraft and H_E and H_P of 1 and 0 respectively to pure electric aircraft. As shown in the Figures, as the power split increases, the range performance of the Hybrid-Electric ATR72-X also increases, but as the energy hybridization increases, the range performance decreases. Also, as the specific battery energy goes higher, the starting energy of the aircraft is also increasing, thus resulting in an increase in range performance for the ATR72-X Hybrid.

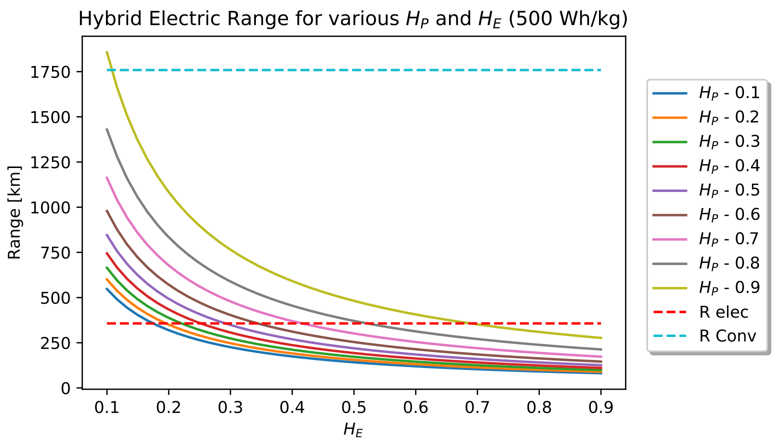

FIGURE 4.3: Range vs Energy Hybridization on various power split for 500 Wh/kg

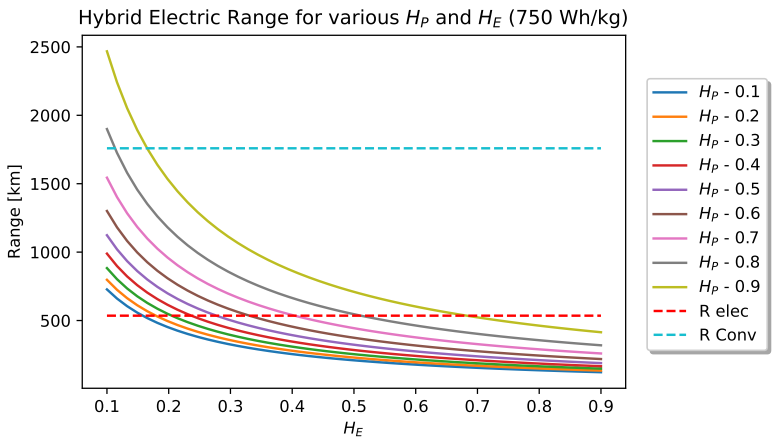

FIGURE 4.4: Range vs Energy Hybridization on various power split for 750 Wh/kg

If we look at the results, the difference between the various specific battery is quite significant, with the highest between each result with H_P of 0.9 almost 500 km. With a specific energy battery of 1000 Wh/kg, it can achieve a high range performance of around 2900 km as shown in Figure 4.5, but it's on the higher power split and higher battery density, which would mean that it would need a very high-power electric motor to produce the results. In this case, the ATR72-X power required for cruising would be around 1.6 MW, so the power split on the hybrid-electrical would be 1.44 MW of electric motor and 0.16 MW of the

Turboprop engine/ICE. With the current technology, it would still not be feasible to use on commercial aircrafts.

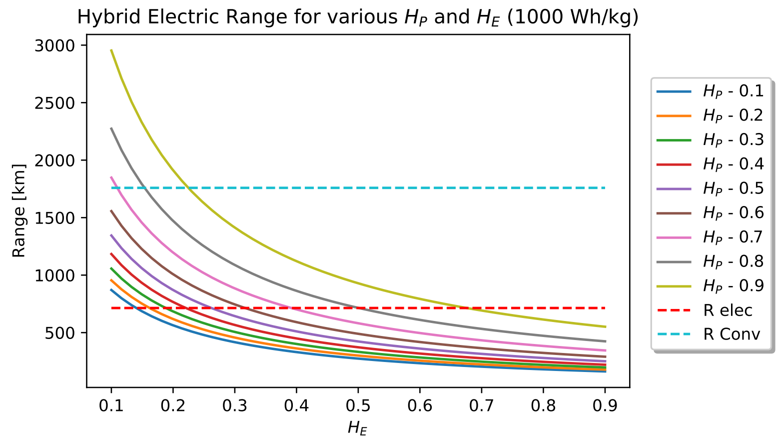

FIGURE 4.5: Range vs Energy Hybridization on various power split for 1000 Wh/kg

The difference between all of the power split (H_p) was quite significant, especially in higher power split. On 1000 Wh/kg shown on Figure 4.5, the difference between 0.9 and 0.8 is around 500 km, and it would decrease as the power split goes lower. So it is possible to convert the aircraft from conventional to hybrid-electric with exactly the same MTOW, but it would need a much higher battery-specific energy and a high-power electrical motor. In many research such as Voskujil et al. **voskuijl_analysis_2018**, De Vries et al. **de_vries_preliminary_2019**, Pornet et al. **pornet_conceptual_2015**, and many more research paper it is better to change the configuration of the aircraft to balance the ratio of fuel and battery weight to produce great range performance or at least maintain the range of the hybrid-electric to that reference aircraft. Although it would be made the aircraft much heavier compared to the reference aircraft, the results will be much more feasible for current technology.

4.3 ATR 72 Hybrid Electric vs Conventional

a

TABLE 4.1: Conventional and Pure Electric Configuration Results

H_P -	H_e -	H_{bat} [J]	M_{bat} [kg]	M_{fuel} [kg]	H_{fuel} [J]	E_{start} [J]	Range [km]
0	0	3.6×10^6	0.000	3414.398	4.32×10^7	4.09×10^7	1758.866
0	1	1.8×10^6	3414.398	0	4.32×10^7	3.41×10^6	387.388
0	1	2.7×10^6	3414.398	0	4.32×10^7	3.41×10^6	581.083
0	1	3.6×10^6	3414.398	0	4.32×10^7	3.41×10^6	774.77

Table 4.1 shows the result of conventional and pure electric aircraft configurations. The blue dashed line and red dashed line in Figure 4.3, 4.4, and 4.5 represent the range performance of the conventional airplane and pure electric, respectively. When comparing the conventional to hybrid-electric with the same configuration (i.e MTOW, Geometry, etc.), the range performance of the Hybrid-Electric configuration for most power split (H_p) would still be lower from the conventional configuration. This is due to the specific energy of the battery being far too low compared to fuel-specific energy unless having a high-power electric motor, high-specific energy battery, or by changing the configuration of the aircraft. Though, if we look into the CO2 emission, the Hybrid-Electrical configuration will produce much lower CO2 emission compared to the conventional configuration and it is achievable for the lower power split of 0.4 and energy hybridization of 0.1 but with around half of the range performance of the aircraft. For a short-range mission, it is very feasible and beneficial.

As for the pure electrical with constant MTOW, the results are still very far compared to the conventional configuration, with only around one-fifth of the range performance for the current battery technology of 500 Wh/kg. It needed to have a high battery density of about 5 times the current technology to compete or at least reach the range of the conventional. However, the 387 kilometers range is still feasible and might benefit a short-distance mission

So in order for the hybrid-electric and pure electric configuration to match the range of conventional, significant improvement in technology would be very much necessary over the next few decades, unless we make adjustments such as increasing the MTOW of the aircraft, changing the aircraft body to a suitable configuration for the needs, or constructing an entirely new aircraft.

4.3.1 Hybrid-electrical range for fuel capacity required of 500 km range ATR72-X

TABLE 4.2: Hybrid-electrical range for fuel capacity required of 500 km range ATR72-X

Parameter	1	2	3	4	5
H_E	0.1	0.1	0.1	0.1	0.1
H_P	0.9	0.7	0.8	0.6	0.7
Battery Capacity [Wh/kg]	500	750	750	1000	1000
Battery mass [kg]	673.791	592.936	592.936	529.407	529.407
Battery mass [lb]	1485.454	1307.200	1307.200	1167.142	1167.142
Fuel mass [kg]	252.671	333.526	333.526	397.055	397.055
Fuel mass [lb]	557.044	735.298	735.298	875.356	875.356
Range [km]	556.15	460.26	566.211	462.27	548.778
Range [nmi]	300.297	248.520	305.729	249.605	296.316

Table 4.2 shows the hybrid-electrical aircraft range result with the fuel capacity required for a 500km range conventional ATR72-X. The fuel capacity of the conventional ATR72-X for a 500 km range requirement is around 926.462 kg.

There are 5 configurations that are comparable to the 500 km conventional ATR72-X. The specific energy of the battery ranges from 500 - 1000 Wh/kg and the composition of the battery mass and fuel mass is shown in the Table. With the current state technology of battery, we could achieve the comparable range from the 500 km conventional ATR72-X without changing the MTOW of the aircraft with the hybrid parameter of H_P of 0.9 and H_E of 0.1 and will be resulting a range of 556.15 km as shown in Table as configuration 1.

CHAPTER 5
SUMMARY, CONCLUSION, RECOMMENDATION

5.1 Summary

The summary of this thesis, which is based on what has been demonstrated and discussed, is as follows:

- The author managed to find and verify the formula for the range performance of the hybrid-electrical propulsion with the constant-power split as the power management of the aircraft;
- The author managed to formulate the battery and fuel estimation for hybrid-electrical aircraft with respect to the existing storage weight configuration;
- This thesis assessed the hybrid-electric ATR72-X range with different hybridization factors such as the Hybridization of power (H_P), and Hybridization of energy (H_E), also the variation of battery-specific energy;
- The author has evaluated the result from the hybrid-electric ATR72-X range and compare it with the conventional configuration ATR72-X;

5.2 Conclusion

The objective of this research is to analyze the range performance of Hybrid-Electrical aircraft. To analyze the range performance, we have to find a formula and calculation as to how to find the range of the Hybrid-Electrical aircraft, as it cannot use the conventional Breguet Range Equation. Thus, in this thesis, we will be using the Hybrid-Electrical range calculation that has been made by Voskujil

voskuijl_analysis_2018. It is a Breguet equation that has been modified to find the range of Hybrid-Electrical aircraft. On Hybrid-Electric there are variables such as H_P and H_E to determine how much ratio of power that are supplied from both power sources, and the ratio of energy sources respectively. Thus, we are analyzing how much those variables are impacting the range performance of Hybrid-Electrical aircraft.

From the results that have been obtained from the research analysis of this thesis, it can be concluded that for a Hybrid-Electrical aircraft as the Hybridization of Power goes higher the range of the aircraft is also increasing. But for Hybridization of Energy (H_E), the higher it goes, it will lower the range of the aircraft. As mentioned in Chapter 4, it was due to the battery-specific energy being much lower than the fuel-specific energy. So when the H_E goes higher, the battery mass will also be increasing, and the fuel mass decrease. And that will be causing the total energy to decrease also because the total energy is related to the total mass of the source times to their specific energy. Thus affecting the range performance of the aircraft. However, it is still achievable if we consider the range of 740 km using H_P of around 0.4 and H_E of about 0.1 for 500 Wh/kg specific battery energy. And from that result, we could use the aircraft for short-range missions with much lower fuel consumption.

For ATR72-X to be converted into Hybrid-Electric Propulsion System (HEPS) with constant MTOW can be beneficial in terms of the overall fuel consumption and CO2 emission with a similar range compared to the conventional configuration. But, the results of the range performance would still fall back, only with the higher power split and low energy hybridization that can be compared to the conventional configuration, such as the result for 1000 Wh/kg with 0.7 of H_P and 0.1 of H_E, but with the current technology, it would be not feasible. The range performance of hybrid-electrical aircraft would be much more feasible if the aircraft configuration is changed rather than no changes in a configuration such as in the papers that have been conducted by Voskujil **voskuijl_analysis_2018**, Pornet and Isikveren **pornet_conceptual_2015**, and many more researcher. But it would be much more complicated and the aircraft's weight will be much heavier.

Overall, it is possible to convert the aircraft to Hybrid-Electrical without changing any configuration to the overall weight of the aircraft, but it would need much more technological advances.

5.3 Recommendation

1. A research on another formula or approach for calculating the range of hybrid electric aircraft while maintaining MTOW.

2. For further topics regarding this thesis, another performance analysis such as take-off, endurance, landing, climbing, etc. for a similar configuration would be recommended.

Appendices

Appendix A: Result

.1 Result for Specific Energy of 500 Wh/kg

Table 1: Hybrid-Electric range with various H_e and H_p of 0.1

H_P	H_e	H_{bat}	M_{bat}	M_{fuel}	H_{fuel}	E_{start}	Range
-	-	[J]	[kg]	[kg]	[J]	[J]	[km]
0.1	0.1	1.8×10^6	1951.085	1463.313	4.32×10^7	44.697×10^9	547.365
0.1	0.2	1.8×10^6	2560.799	853.600	4.32×10^7	26.339×10^9	319.420
0.1	0.3	1.8×10^6	2858.566	555.832	4.32×10^7	18.671×10^9	225.513
0.1	0.4	1.8×10^6	3035.020	379.378	4.32×10^7	14.460×10^9	174.278
0.1	0.5	1.8×10^6	3151.752	262.646	4.32×10^7	11.800×10^9	142.013
0.1	0.6	1.8×10^6	3234.693	179.705	4.32×10^7	9.966×10^9	119.829
0.1	0.7	1.8×10^6	3296.660	117.738	4.32×10^7	8.626×10^9	103.640
0.1	0.8	1.8×10^6	3344.716	69.682	4.32×10^7	7.603×10^9	91.304
0.1	0.9	1.8×10^6	3383.073	31.325	4.32×10^7	6.797×10^9	81.592

Table 2: Hybrid-Electric range with various H_e and H_p of 0.2

H_P -	H_e -	H_{bat} [J]	M_{bat} [kg]	M_{fuel} [kg]	H_{fuel} [J]	E_{start} [J]	Range [km]
0.2	0.1	$1.8{\times}10^6$	1951.085	1463.313	$4.32{\times}10^7$	$44.697{\times}10^9$	600.283
0.2	0.2	$1.8{\times}10^6$	2560.799	853.600	$4.32{\times}10^7$	$26.339{\times}10^9$	350.301
0.2	0.3	$1.8{\times}10^6$	2858.566	555.832	$4.32{\times}10^7$	$18.671{\times}10^9$	247.315
0.2	0.4	$1.8{\times}10^6$	3035.020	379.378	$4.32{\times}10^7$	$14.460{\times}10^9$	191.126
0.2	0.5	$1.8{\times}10^6$	3151.752	262.646	$4.32{\times}10^7$	$11.800{\times}10^9$	155.743
0.2	0.6	$1.8{\times}10^6$	3234.693	179.705	$4.32{\times}10^7$	$9.966{\times}10^9$	131.414
0.2	0.7	$1.8{\times}10^6$	3296.660	117.738	$4.32{\times}10^7$	$8.626{\times}10^9$	113.659
0.2	0.8	$1.8{\times}10^6$	3344.716	69.682	$4.32{\times}10^7$	$7.603{\times}10^9$	100.131
0.2	0.9	$1.8{\times}10^6$	3383.073	31.325	$4.32{\times}10^7$	$6.797{\times}10^9$	89.481

Table 3: Hybrid-Electric range with various H_e and H_p of 0.3

H_P -	H_e -	H_{bat} [J]	M_{bat} [kg]	M_{fuel} [kg]	H_{fuel} [J]	E_{start} [J]	Range [km]
0.3	0.1	$1.8{\times}10^6$	1951.085	1463.313	$4.32{\times}10^7$	$44.697{\times}10^9$	664.528
0.3	0.2	$1.8{\times}10^6$	2560.799	853.600	$4.32{\times}10^7$	$26.339{\times}10^9$	387.791
0.3	0.3	$1.8{\times}10^6$	2858.566	555.832	$4.32{\times}10^7$	$18.671{\times}10^9$	273.784
0.3	0.4	$1.8{\times}10^6$	3035.020	379.378	$4.32{\times}10^7$	$14.460{\times}10^9$	211.582
0.3	0.5	$1.8{\times}10^6$	3151.752	262.646	$4.32{\times}10^7$	$11.800{\times}10^9$	172.411
0.3	0.6	$1.8{\times}10^6$	3234.693	179.705	$4.32{\times}10^7$	$9.966{\times}10^9$	145.479
0.3	0.7	$1.8{\times}10^6$	3296.660	117.738	$4.32{\times}10^7$	$8.626{\times}10^9$	125.824
0.3	0.8	$1.8{\times}10^6$	3344.716	69.682	$4.32{\times}10^7$	$7.603{\times}10^9$	110.847
0.3	0.9	$1.8{\times}10^6$	3383.073	31.325	$4.32{\times}10^7$	$6.797{\times}10^9$	99.057
0.3	0.9	$1.8{\times}10^6$	3383.073	31.325	$4.32{\times}10^7$	$6.797{\times}10^9$	0.996

TABLE 4: Hybrid-Electric range with various H_e and H_p of 0.4

H_P -	H_e -	H_{bat} [J]	M_{bat} [kg]	M_{fuel} [kg]	H_{fuel} [J]	E_{start} [J]	Range [km]
0.4	0.1	1.8×10^6	1951.085	1463.313	4.32×10^7	44.697×10^9	744.173
0.4	0.2	1.8×10^6	2560.799	853.600	4.32×10^7	26.339×10^9	434.269
0.4	0.3	1.8×10^6	2858.566	555.832	4.32×10^7	18.671×10^9	306.597
0.4	0.4	1.8×10^6	3035.020	379.378	4.32×10^7	14.460×10^9	236.940
0.4	0.5	1.8×10^6	3151.752	262.646	4.32×10^7	11.800×10^9	193.075
0.4	0.6	1.8×10^6	3234.693	179.705	4.32×10^7	9.966×10^9	162.914
0.4	0.7	1.8×10^6	3296.660	117.738	4.32×10^7	8.626×10^9	140.904
0.4	0.8	1.8×10^6	3344.716	69.682	4.32×10^7	7.603×10^9	124.133
0.4	0.9	1.8×10^6	3383.073	31.325	4.32×10^7	6.797×10^9	110.929

TABLE 5: Hybrid-Electric range with various H_e and H_p of 0.5

H_P -	H_e -	H_{bat} [J]	M_{bat} [kg]	M_{fuel} [kg]	H_{fuel} [J]	E_{start} [J]	Range [km]
0.5	0.1	1.8×10^6	1951.085	1463.313	4.32×10^7	44.697×10^9	845.508
0.5	0.2	1.8×10^6	2560.799	853.600	4.32×10^7	26.339×10^9	493.404
0.5	0.3	1.8×10^6	2858.566	555.832	4.32×10^7	18.671×10^9	348.347
0.5	0.4	1.8×10^6	3035.020	379.378	4.32×10^7	14.460×10^9	269.204
0.5	0.5	1.8×10^6	3151.752	262.646	4.32×10^7	11.800×10^9	219.366
0.5	0.6	1.8×10^6	3234.693	179.705	4.32×10^7	9.966×10^9	185.099
0.5	0.7	1.8×10^6	3296.660	117.738	4.32×10^7	8.626×10^9	160.091
0.5	0.8	1.8×10^6	3344.716	69.682	4.32×10^7	7.603×10^9	141.036
0.5	0.9	1.8×10^6	3383.073	31.325	4.32×10^7	6.797×10^9	126.035

TABLE 6: Hybrid-Electric range with various H_e and H_p of 0.6

H_P -	H_e -	H_{bat} [J]	M_{bat} [kg]	M_{fuel} [kg]	H_{fuel} [J]	E_{start} [J]	Range [km]
0.6	0.1	1.8×10^6	1951.085	1463.313	4.32×10^7	44.697×10^9	978.791
0.6	0.2	1.8×10^6	2560.799	853.600	4.32×10^7	26.339×10^9	571.182
0.6	0.3	1.8×10^6	2858.566	555.832	4.32×10^7	18.671×10^9	403.259
0.6	0.4	1.8×10^6	3035.020	379.378	4.32×10^7	14.460×10^9	311.641
0.6	0.5	1.8×10^6	3151.752	262.646	4.32×10^7	11.800×10^9	253.946
0.6	0.6	1.8×10^6	3234.693	179.705	4.32×10^7	9.966×10^9	214.277
0.6	0.7	1.8×10^6	3296.660	117.738	4.32×10^7	8.626×10^9	185.327
0.6	0.8	1.8×10^6	3344.716	69.682	4.32×10^7	7.603×10^9	163.269
0.6	0.9	1.8×10^6	3383.073	31.325	4.32×10^7	6.797×10^9	145.903

TABLE 7: Hybrid-Electric range with various H_e and H_p of 0.7

H_P -	H_e -	H_{bat} [J]	M_{bat} [kg]	M_{fuel} [kg]	H_{fuel} [J]	E_{start} [J]	Range [km]
0.7	0.1	1.8×10^6	1951.085	1463.313	4.32×10^7	44.697×10^9	1161.959
0.7	0.2	1.8×10^6	2560.799	853.600	4.32×10^7	26.339×10^9	678.072
0.7	0.3	1.8×10^6	2858.566	555.832	4.32×10^7	18.671×10^9	478.724
0.7	0.4	1.8×10^6	3035.020	379.378	4.32×10^7	14.460×10^9	369.961
0.7	0.5	1.8×10^6	3151.752	262.646	4.32×10^7	11.800×10^9	301.469
0.7	0.6	1.8×10^6	3234.693	179.705	4.32×10^7	9.966×10^9	254.376
0.7	0.7	1.8×10^6	3296.660	117.738	4.32×10^7	8.626×10^9	220.009
0.7	0.8	1.8×10^6	3344.716	69.682	4.32×10^7	7.603×10^9	193.822
0.7	0.9	1.8×10^6	3383.073	31.325	4.32×10^7	6.797×10^9	173.206

TABLE 8: Hybrid-Electric range with various H_e and H_p of 0.8

H_P -	H_e -	H_{bat} [J]	M_{bat} [kg]	M_{fuel} [kg]	H_{fuel} [J]	E_{start} [J]	Range [km]
0.8	0.1	1.8×10^6	1951.085	1463.313	4.32×10^7	44.697×10^9	1429.465
0.8	0.2	1.8×10^6	2560.799	853.600	4.32×10^7	26.339×10^9	834.177
0.8	0.3	1.8×10^6	2858.566	555.832	4.32×10^7	18.671×10^9	588.936
0.8	0.4	1.8×10^6	3035.020	379.378	4.32×10^7	14.460×10^9	455.133
0.8	0.5	1.8×10^6	3151.752	262.646	4.32×10^7	11.800×10^9	370.873
0.8	0.6	1.8×10^6	3234.693	179.705	4.32×10^7	9.966×10^9	312.939
0.8	0.7	1.8×10^6	3296.660	117.738	4.32×10^7	8.626×10^9	270.659
0.8	0.8	1.8×10^6	3344.716	69.682	4.32×10^7	7.603×10^9	238.444
0.8	0.9	1.8×10^6	3383.073	31.325	4.32×10^7	6.797×10^9	213.082

TABLE 9: Hybrid-Electric range with various H_e and H_p of 0.9

H_P -	H_e -	H_{bat} [J]	M_{bat} [kg]	M_{fuel} [kg]	H_{fuel} [J]	E_{start} [J]	Range [km]
0.9	0.1	1.8×10^6	1951.085	1463.313	4.32×10^7	44.697×10^9	1856.978
0.9	0.2	1.8×10^6	2560.799	853.600	4.32×10^7	26.339×10^9	1083.656
0.9	0.3	1.8×10^6	2858.566	555.832	4.32×10^7	18.671×10^9	765.070
0.9	0.4	1.8×10^6	3035.020	379.378	4.32×10^7	14.460×10^9	591.251
0.9	0.5	1.8×10^6	3151.752	262.646	4.32×10^7	11.800×10^9	481.791
0.9	0.6	1.8×10^6	3234.693	179.705	4.32×10^7	9.966×10^9	406.530
0.9	0.7	1.8×10^6	3296.660	117.738	4.32×10^7	8.626×10^9	351.606
0.9	0.8	1.8×10^6	3344.716	69.682	4.32×10^7	7.603×10^9	309.756
0.9	0.9	1.8×10^6	3383.073	31.325	4.32×10^7	6.797×10^9	276.809

.2 Result for Specific Energy of 750 Wh/kg

TABLE 10: Hybrid-Electric range with various H_e and H_p of 0.1

H_P -	H_e -	H_{bat} [J]	M_{bat} [kg]	M_{fuel} [kg]	H_{fuel} [J]	E_{start} [J]	Range [km]
0.1	0.1	2.7×10^6	1951.085	1463.313	4.32×10^7	59×10^9	727.346
0.1	0.2	2.7×10^6	2560.799	853.600	4.32×10^7	36.875×10^9	449.105
0.1	0.3	2.7×10^6	2858.566	555.832	4.32×10^7	26.818×10^9	324.850
0.1	0.4	2.7×10^6	3035.020	379.378	4.32×10^7	21.071×10^9	254.453
0.1	0.5	2.7×10^6	3151.752	262.646	4.32×10^7	17.353×10^9	209.133
0.1	0.6	2.7×10^6	3234.693	179.705	4.32×10^7	14.750×10^9	177.517
0.1	0.7	2.7×10^6	3296.660	117.738	4.32×10^7	12.826×10^9	154.204
0.1	0.8	2.7×10^6	3344.716	69.682	4.32×10^7	11.346×10^9	136.304
0.1	0.9	2.7×10^6	3383.073	31.325	4.32×10^7	10.172×10^9	122.128

TABLE 11: Hybrid-Electric range with various H_e and H_p of 0.2

H_P -	H_e -	H_{bat} [J]	M_{bat} [kg]	M_{fuel} [kg]	H_{fuel} [J]	E_{start} [J]	Range [km]
0.2	0.1	2.7×10^6	1951.085	1463.313	4.32×10^7	59×10^9	797.663
0.2	0.2	2.7×10^6	2560.799	853.600	4.32×10^7	36.875×10^9	492.523
0.2	0.3	2.7×10^6	2858.566	555.832	4.32×10^7	26.818×10^9	356.256
0.2	0.4	2.7×10^6	3035.020	379.378	4.32×10^7	21.071×10^9	279.053
0.2	0.5	2.7×10^6	3151.752	262.646	4.32×10^7	17.353×10^9	229.352
0.2	0.6	2.7×10^6	3234.693	179.705	4.32×10^7	14.750×10^9	194.679
0.2	0.7	2.7×10^6	3296.660	117.738	4.32×10^7	12.826×10^9	169.113
0.2	0.8	2.7×10^6	3344.716	69.682	4.32×10^7	11.346×10^9	149.482
0.2	0.9	2.7×10^6	3383.073	31.325	4.32×10^7	10.172×10^9	133.935

Table 12: Hybrid-Electric range with various H_e and H_p of 0.3

H_P -	H_e -	H_{bat} [J]	M_{bat} [kg]	M_{fuel} [kg]	H_{fuel} [J]	E_{start} [J]	Range [km]
0.3	0.1	2.7×10^6	1951.085	1463.313	4.32×10^7	59×10^9	883.033
0.3	0.2	2.7×10^6	2560.799	853.600	4.32×10^7	36.875×10^9	545.235
0.3	0.3	2.7×10^6	2858.566	555.832	4.32×10^7	26.818×10^9	394.384
0.3	0.4	2.7×10^6	3035.020	379.378	4.32×10^7	21.071×10^9	308.918
0.3	0.5	2.7×10^6	3151.752	262.646	4.32×10^7	17.353×10^9	253.898
0.3	0.6	2.7×10^6	3234.693	179.705	4.32×10^7	14.750×10^9	215.514
0.3	0.7	2.7×10^6	3296.660	117.738	4.32×10^7	12.826×10^9	187.212
0.3	0.8	2.7×10^6	3344.716	69.682	4.32×10^7	11.346×10^9	165.480
0.3	0.9	2.7×10^6	3383.073	31.325	4.32×10^7	10.172×10^9	148.269

Table 13: Hybrid-Electric range with various H_e and H_p of 0.4

H_P -	H_e -	H_{bat} [J]	M_{bat} [kg]	M_{fuel} [kg]	H_{fuel} [J]	E_{start} [J]	Range [km]
0.4	0.1	2.7×10^6	1951.085	1463.313	4.32×10^7	59×10^9	988.865
0.4	0.2	2.7×10^6	2560.799	853.600	4.32×10^7	36.875×10^9	610.582
0.4	0.3	2.7×10^6	2858.566	555.832	4.32×10^7	26.818×10^9	441.651
0.4	0.4	2.7×10^6	3035.020	379.378	4.32×10^7	21.071×10^9	345.943
0.4	0.5	2.7×10^6	3151.752	262.646	4.32×10^7	17.353×10^9	284.328
0.4	0.6	2.7×10^6	3234.693	179.705	4.32×10^7	14.750×10^9	241.344
0.4	0.7	2.7×10^6	3296.660	117.738	4.32×10^7	12.826×10^9	209.649
0.4	0.8	2.7×10^6	3344.716	69.682	4.32×10^7	11.346×10^9	185.313
0.4	0.9	2.7×10^6	3383.073	31.325	4.32×10^7	10.172×10^9	166.039

TABLE 14: Hybrid-Electric range with various H_e and H_p of 0.5

H_P -	H_e -	H_{bat} [J]	M_{bat} [kg]	M_{fuel} [kg]	H_{fuel} [J]	E_{start} [J]	Range [km]
0.5	0.1	2.7×10^6	1951.085	1463.313	4.32×10^7	59×10^9	1123.521
0.5	0.2	2.7×10^6	2560.799	853.600	4.32×10^7	36.875×10^9	693.726
0.5	0.3	2.7×10^6	2858.566	555.832	4.32×10^7	26.818×10^9	501.791
0.5	0.4	2.7×10^6	3035.020	379.378	4.32×10^7	21.071×10^9	393.050
0.5	0.5	2.7×10^6	3151.752	262.646	4.32×10^7	17.353×10^9	323.045
0.5	0.6	2.7×10^6	3234.693	179.705	4.32×10^7	14.750×10^9	274.208
0.5	0.7	2.7×10^6	3296.660	117.738	4.32×10^7	12.826×10^9	238.198
0.5	0.8	2.7×10^6	3344.716	69.682	4.32×10^7	11.346×10^9	210.548
0.5	0.9	2.7×10^6	3383.073	31.325	4.32×10^7	10.172×10^9	188.649

TABLE 15: Hybrid-Electric range with various H_e and H_p of 0.6

H_P -	H_e -	H_{bat} [J]	M_{bat} [kg]	M_{fuel} [kg]	H_{fuel} [J]	E_{start} [J]	Range [km]
0.6	0.1	2.7×10^6	1951.085	1463.313	4.32×10^7	59×10^9	1300.629
0.6	0.2	2.7×10^6	2560.799	853.600	4.32×10^7	36.875×10^9	803.083
0.6	0.3	2.7×10^6	2858.566	555.832	4.32×10^7	26.818×10^9	580.893
0.6	0.4	2.7×10^6	3035.020	379.378	4.32×10^7	21.071×10^9	455.009
0.6	0.5	2.7×10^6	3151.752	262.646	4.32×10^7	17.353×10^9	373.969
0.6	0.6	2.7×10^6	3234.693	179.705	4.32×10^7	14.750×10^9	317.433
0.6	0.7	2.7×10^6	3296.660	117.738	4.32×10^7	12.826×10^9	275.746
0.6	0.8	2.7×10^6	3344.716	69.682	4.32×10^7	11.346×10^9	243.738
0.6	0.9	2.7×10^6	3383.073	31.325	4.32×10^7	10.172×10^9	218.387

Table 16: Hybrid-Electric range with various H_e and H_p of 0.7

H_P -	H_e -	H_{bat} [J]	M_{bat} [kg]	M_{fuel} [kg]	H_{fuel} [J]	E_{start} [J]	Range [km]
0.7	0.1	2.7×10^6	1951.085	1463.313	4.32×10^7	59×10^9	1544.025
0.7	0.2	2.7×10^6	2560.799	853.600	4.32×10^7	36.875×10^9	953.370
0.7	0.3	2.7×10^6	2858.566	555.832	4.32×10^7	26.818×10^9	689.599
0.7	0.4	2.7×10^6	3035.020	379.378	4.32×10^7	21.071×10^9	540.159
0.7	0.5	2.7×10^6	3151.752	262.646	4.32×10^7	17.353×10^9	443.953
0.7	0.6	2.7×10^6	3234.693	179.705	4.32×10^7	14.750×10^9	376.837
0.7	0.7	2.7×10^6	3296.660	117.738	4.32×10^7	12.826×10^9	327.349
0.7	0.8	2.7×10^6	3344.716	69.682	4.32×10^7	11.346×10^9	289.350
0.7	0.9	2.7×10^6	3383.073	31.325	4.32×10^7	10.172×10^9	259.256

Table 17: Hybrid-Electric range with various H_e and H_p of 0.8

H_P -	H_e -	H_{bat} [J]	M_{bat} [kg]	M_{fuel} [kg]	H_{fuel} [J]	E_{start} [J]	Range [km]
0.8	0.1	2.7×10^6	1951.085	1463.313	4.32×10^7	59×10^9	1899.491
0.8	0.2	2.7×10^6	2560.799	853.600	4.32×10^7	36.875×10^9	1172.854
0.8	0.3	2.7×10^6	2858.566	555.832	4.32×10^7	26.818×10^9	848.358
0.8	0.4	2.7×10^6	3035.020	379.378	4.32×10^7	21.071×10^9	664.514
0.8	0.5	2.7×10^6	3151.752	262.646	4.32×10^7	17.353×10^9	546.160
0.8	0.6	2.7×10^6	3234.693	179.705	4.32×10^7	14.750×10^9	463.592
0.8	0.7	2.7×10^6	3296.660	117.738	4.32×10^7	12.826×10^9	402.711
0.8	0.8	2.7×10^6	3344.716	69.682	4.32×10^7	11.346×10^9	355.964
0.8	0.9	2.7×10^6	3383.073	31.325	4.32×10^7	10.172×10^9	318.942

TABLE 18: Hybrid-Electric range with various H_e and H_p of 0.9

H_P -	H_e -	H_{bat} [J]	M_{bat} [kg]	M_{fuel} [kg]	H_{fuel} [J]	E_{start} [J]	Range [km]
0.9	0.1	2.7×10^6	1951.085	1463.313	4.32×10^7	59×10^9	2467.575
0.9	0.2	2.7×10^6	2560.799	853.600	4.32×10^7	36.875×10^9	1523.622
0.9	0.3	2.7×10^6	2858.566	555.832	4.32×10^7	26.818×10^9	1102.079
0.9	0.4	2.7×10^6	3035.020	379.378	4.32×10^7	21.071×10^9	863.251
0.9	0.5	2.7×10^6	3151.752	262.646	4.32×10^7	17.353×10^9	709.501
0.9	0.6	2.7×10^6	3234.693	179.705	4.32×10^7	14.750×10^9	602.239
0.9	0.7	2.7×10^6	3296.660	117.738	4.32×10^7	12.826×10^9	523.150
0.9	0.8	2.7×10^6	3344.716	69.682	4.32×10^7	11.346×10^9	462.423
0.9	0.9	2.7×10^6	3383.073	31.325	4.32×10^7	10.172×10^9	414.328

.3 Result for Specific Energy of 1000 Wh/kg

TABLE 19: Hybrid-Electric range with various H_e and H_p of 0.1

H_P -	H_e -	H_{bat} [J]	M_{bat} [kg]	M_{fuel} [kg]	H_{fuel} [J]	E_{start} [J]	Range [km]
0.1	0.1	3.6×10^6	1951.085	1463.313	4.32×10^7	70.239×10^9	870.472
0.1	0.2	3.6×10^6	2560.799	853.600	4.32×10^7	46.094×10^9	563.500
0.1	0.3	3.6×10^6	2858.566	555.832	4.32×10^7	34.302×10^9	416.608
0.1	0.4	3.6×10^6	3035.020	379.378	4.32×10^7	27.315×10^9	330.468
0.1	0.5	3.6×10^6	3151.752	262.646	4.32×10^7	22.692×10^9	273.848
0.1	0.6	3.6×10^6	3234.693	179.705	4.32×10^7	19.408×10^9	233.792
0.1	0.7	3.6×10^6	3296.660	117.738	4.32×10^7	16.954×10^9	203.959
0.1	0.8	3.6×10^6	3344.716	69.682	4.32×10^7	15.051×10^9	180.879
0.1	0.9	3.6×10^6	3383.073	31.325	4.32×10^7	13.532×10^9	162.491

Table 20: Hybrid-Electric range with various H_e and H_p of 0.2

H_P -	H_e -	H_{bat} [J]	M_{bat} [kg]	M_{fuel} [kg]	H_{fuel} [J]	E_{start} [J]	Range [km]
0.2	0.1	3.6×10^6	1951.085	1463.313	4.32×10^7	70.239×10^9	954.627
0.2	0.2	3.6×10^6	2560.799	853.600	4.32×10^7	46.094×10^9	617.978
0.2	0.3	3.6×10^6	2858.566	555.832	4.32×10^7	34.302×10^9	456.885
0.2	0.4	3.6×10^6	3035.020	379.378	4.32×10^7	27.315×10^9	362.417
0.2	0.5	3.6×10^6	3151.752	262.646	4.32×10^7	22.692×10^9	300.323
0.2	0.6	3.6×10^6	3234.693	179.705	4.32×10^7	19.408×10^9	256.395
0.2	0.7	3.6×10^6	3296.660	117.738	4.32×10^7	16.954×10^9	223.678
0.2	0.8	3.6×10^6	3344.716	69.682	4.32×10^7	15.051×10^9	198.366
0.2	0.9	3.6×10^6	3383.073	31.325	4.32×10^7	13.532×10^9	178.200

Table 21: Hybrid-Electric range with various H_e and H_p of 0.3

H_P -	H_e -	H_{bat} [J]	M_{bat} [kg]	M_{fuel} [kg]	H_{fuel} [J]	E_{start} [J]	Range [km]
0.3	0.1	3.6×10^6	1951.085	1463.313	4.32×10^7	70.239×10^9	1056.795
0.3	0.2	3.6×10^6	2560.799	853.600	4.32×10^7	46.094×10^9	684.116
0.3	0.3	3.6×10^6	2858.566	555.832	4.32×10^7	34.302×10^9	505.783
0.3	0.4	3.6×10^6	3035.020	379.378	4.32×10^7	27.315×10^9	401.205
0.3	0.5	3.6×10^6	3151.752	262.646	4.32×10^7	22.692×10^9	332.465
0.3	0.6	3.6×10^6	3234.693	179.705	4.32×10^7	19.408×10^9	283.835
0.3	0.7	3.6×10^6	3296.660	117.738	4.32×10^7	16.954×10^9	247.617
0.3	0.8	3.6×10^6	3344.716	69.682	4.32×10^7	15.051×10^9	219.596
0.3	0.9	3.6×10^6	3383.073	31.325	4.32×10^7	13.532×10^9	197.272

Table 22: Hybrid-Electric range with various H_e and H_p of 0.4

H_P -	H_e -	H_{bat} [J]	M_{bat} [kg]	M_{fuel} [kg]	H_{fuel} [J]	E_{start} [J]	Range [km]
0.4	0.1	3.6×10^6	1951.085	1463.313	4.32×10^7	70.239×10^9	1183.453
0.4	0.2	3.6×10^6	2560.799	853.600	4.32×10^7	46.094×10^9	766.109
0.4	0.3	3.6×10^6	2858.566	555.832	4.32×10^7	34.302×10^9	566.402
0.4	0.4	3.6×10^6	3035.020	379.378	4.32×10^7	27.315×10^9	449.290
0.4	0.5	3.6×10^6	3151.752	262.646	4.32×10^7	22.692×10^9	372.311
0.4	0.6	3.6×10^6	3234.693	179.705	4.32×10^7	19.408×10^9	317.853
0.4	0.7	3.6×10^6	3296.660	117.738	4.32×10^7	16.954×10^9	277.294
0.4	0.8	3.6×10^6	3344.716	69.682	4.32×10^7	15.051×10^9	245.914
0.4	0.9	3.6×10^6	3383.073	31.325	4.32×10^7	13.532×10^9	220.915

Table 23: Hybrid-Electric range with various H_e and H_p of 0.5

H_P -	H_e -	H_{bat} [J]	M_{bat} [kg]	M_{fuel} [kg]	H_{fuel} [J]	E_{start} [J]	Range [km]
0.5	0.1	3.6×10^6	1951.085	1463.313	4.32×10^7	70.239×10^9	1344.606
0.5	0.2	3.6×10^6	2560.799	853.600	4.32×10^7	46.094×10^9	870.431
0.5	0.3	3.6×10^6	2858.566	555.832	4.32×10^7	34.302×10^9	643.529
0.5	0.4	3.6×10^6	3035.020	379.378	4.32×10^7	27.315×10^9	510.470
0.5	0.5	3.6×10^6	3151.752	262.646	4.32×10^7	22.692×10^9	423.009
0.5	0.6	3.6×10^6	3234.693	179.705	4.32×10^7	19.408×10^9	361.136
0.5	0.7	3.6×10^6	3296.660	117.738	4.32×10^7	16.954×10^9	315.053
0.5	0.8	3.6×10^6	3344.716	69.682	4.32×10^7	15.051×10^9	279.401
0.5	0.9	3.6×10^6	3383.073	31.325	4.32×10^7	13.532×10^9	250.997

Table 24: Hybrid-Electric range with various H_e and H_p of 0.6

H_P	H_e	H_{bat}	M_{bat}	M_{fuel}	H_{fuel}	E_{start}	Range
-	-	[J]	[kg]	[kg]	[J]	[J]	[km]
0.6	0.1	3.6×10^6	1951.085	1463.313	4.32×10^7	70.239×10^9	1556.566
0.6	0.2	3.6×10^6	2560.799	853.600	4.32×10^7	46.094×10^9	1007.643
0.6	0.3	3.6×10^6	2858.566	555.832	4.32×10^7	34.302×10^9	744.974
0.6	0.4	3.6×10^6	3035.020	379.378	4.32×10^7	27.315×10^9	590.939
0.6	0.5	3.6×10^6	3151.752	262.646	4.32×10^7	22.692×10^9	489.691
0.6	0.6	3.6×10^6	3234.693	179.705	4.32×10^7	19.408×10^9	418.064
0.6	0.7	3.6×10^6	3296.660	117.738	4.32×10^7	16.954×10^9	364.717
0.6	0.8	3.6×10^6	3344.716	69.682	4.32×10^7	15.051×10^9	323.445
0.6	0.9	3.6×10^6	3383.073	31.325	4.32×10^7	13.532×10^9	290.564

Table 25: Hybrid-Electric range with various H_e and H_p of 0.7

H_P	H_e	H_{bat}	M_{bat}	M_{fuel}	H_{fuel}	E_{start}	Range
-	-	[J]	[kg]	[kg]	[J]	[J]	[km]
0.7	0.1	3.6×10^6	1951.085	1463.313	4.32×10^7	70.239×10^9	1847.857
0.7	0.2	3.6×10^6	2560.799	853.600	4.32×10^7	46.094×10^9	1196.211
0.7	0.3	3.6×10^6	2858.566	555.832	4.32×10^7	34.302×10^9	884.386
0.7	0.4	3.6×10^6	3035.020	379.378	4.32×10^7	27.315×10^9	701.526
0.7	0.5	3.6×10^6	3151.752	262.646	4.32×10^7	22.692×10^9	581.331
0.7	0.6	3.6×10^6	3234.693	179.705	4.32×10^7	19.408×10^9	496.299
0.7	0.7	3.6×10^6	3296.660	117.738	4.32×10^7	16.954×10^9	432.970
0.7	0.8	3.6×10^6	3344.716	69.682	4.32×10^7	15.051×10^9	383.973
0.7	0.9	3.6×10^6	3383.073	31.325	4.32×10^7	13.532×10^9	344.939

TABLE 26: Hybrid-Electric range with various H_e and H_p of 0.8

H_P -	H_e -	H_{bat} [J]	M_{bat} [kg]	M_{fuel} [kg]	H_{fuel} [J]	E_{start} [J]	Range [km]
0.8	0.1	3.6×10^6	1951.085	1463.313	4.32×10^7	70.239×10^9	2273.270
0.8	0.2	3.6×10^6	2560.799	853.600	4.32×10^7	46.094×10^9	1471.602
0.8	0.3	3.6×10^6	2858.566	555.832	4.32×10^7	34.302×10^9	1087.989
0.8	0.4	3.6×10^6	3035.020	379.378	4.32×10^7	27.315×10^9	863.031
0.8	0.5	3.6×10^6	3151.752	262.646	4.32×10^7	22.692×10^9	715.165
0.8	0.6	3.6×10^6	3234.693	179.705	4.32×10^7	19.408×10^9	610.557
0.8	0.7	3.6×10^6	3296.660	117.738	4.32×10^7	16.954×10^9	532.648
0.8	0.8	3.6×10^6	3344.716	69.682	4.32×10^7	15.051×10^9	472.372
0.8	0.9	3.6×10^6	3383.073	31.325	4.32×10^7	13.532×10^9	424.351

TABLE 27: Hybrid-Electric range with various H_e and H_p of 0.9

H_P -	H_e -	H_{bat} [J]	M_{bat} [kg]	M_{fuel} [kg]	H_{fuel} [J]	E_{start} [J]	Range [km]
0.9	0.1	3.6×10^6	1951.085	1463.313	4.32×10^7	70.239×10^9	2953.142
0.9	0.2	3.6×10^6	2560.799	853.600	4.32×10^7	46.094×10^9	1911.717
0.9	0.3	3.6×10^6	2858.566	555.832	4.32×10^7	34.302×10^9	1413.376
0.9	0.4	3.6×10^6	3035.020	379.378	4.32×10^7	27.315×10^9	1121.139
0.9	0.5	3.6×10^6	3151.752	262.646	4.32×10^7	22.692×10^9	929.050
0.9	0.6	3.6×10^6	3234.693	179.705	4.32×10^7	19.408×10^9	793.158
0.9	0.7	3.6×10^6	3296.660	117.738	4.32×10^7	16.954×10^9	691.948
0.9	0.8	3.6×10^6	3344.716	69.682	4.32×10^7	15.051×10^9	613.645
0.9	0.9	3.6×10^6	3383.073	31.325	4.32×10^7	13.532×10^9	551.263

Curriculum Vitae

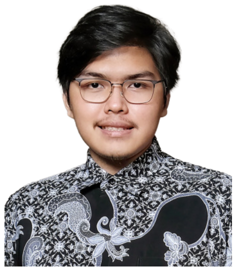

	Basic Information
Name	Reyhan Athalla
Place of Birth	Tangerang,Indonesia
Date of Birth	01, 07, 2001
Address	Anggrek Loka, Tangerang Selatan, Banten, Indonesia
Year	**Education**
2019 - present	International University Liaison Indonesia
2016 - 2019	State Senior High School 2 South Tangerang City
Year	**Seminars & Workshops**
2021	Basic Aircraft Maintenance Training
Year	**Organizational Experiences**
2020-2021	Chairman of IULI General Election Committee
2021-2022	Head of Event Management in Aviation Engineering Student Association